

# MASTER THESIS

## HOW GENOMES ARE SHAPED BY DIRECT AND INDIRECT SELECTION PRESSURE: A STUDY IN IN SILICO EXPERIMENTAL EVOLUTION

BRIAN DAVIS

SUPERVISORS:

BÉRÉNICE BATUT AND ANIKA ERXLEBEN

MAY 2020



ALBERT-LUDWIGS UNIVERSITÄT FREIBURG

BIOINFORMATICS GROUP

PROFESSOR DR. ROLF BACKOFEN

# Abstract

Not all aspects of evolution are fully understood, and one area of pressing interest is reductive evolution, in which the genome of a species evolves to become significantly smaller over time. Among the more well-known examples of this phenomena is *Prochlorococcus*, a marine cyanobacteria whose genome has reduced up to 43% among some of its own ecotypes and around 36% smaller than some strains of its closest living relative, *Synechococcus*. To study the mechanisms behind reductive evolution in the lab would be too difficult, expensive, and above all, slow, so instead *in silico* evolution may be used to study this phenomenon. This method seeks to simulate organisms and their evolution in software, allowing for greater control of the environment, mutation rates, and other variables, as well as providing a full phylogenetic record of all organisms in a lineage. In this thesis the *in silico* tool Aevol is used to study reductive evolution, particularly by looking at how varying one parameter at a time (e.g. mutation and selection rates, population size) impacts the structure of the genome as well as measures such as robustness, evolvability, and fitness. Through these methods, a little light is shed on some of the underlying mechanisms which might lead to reductive evolution. These experiments suggest that effective population size,  $N_e$ , is among the strongest determining factors when it comes to reductive evolution.

# Contents

<b>Abstract</b>	<b>I</b>
<b>List of Figures</b>	<b>III</b>
<b>List of Tables</b>	<b>VI</b>
<b>1 Introduction</b>	<b>1</b>
<b>2 Background</b>	<b>7</b>
2.1 Properties of Genomes . . . . .	7
2.1.1 Evolvability . . . . .	7
2.1.2 Robustness and Antirobustness . . . . .	8
2.1.3 Fitness . . . . .	9
2.2 Reductive Evolution . . . . .	9
2.3 Experimental Evolution . . . . .	10
2.4 Aevol . . . . .	11
2.4.1 Why use Aevol . . . . .	11
2.4.2 Aevol's Architecture . . . . .	12
2.5 Analyzing with Aevol . . . . .	17
2.6 Related Work . . . . .	18
2.6.1 Reductive Evolution . . . . .	18
2.6.2 Investigations in Experimental Evolution . . . . .	20
2.7 Summary . . . . .	21

<b>3 Methods</b>	<b>22</b>
3.1 Contributions . . . . .	22
3.2 Experimental Designs . . . . .	22
3.2.1 Inputs . . . . .	25
3.3 Evaluation Strategy . . . . .	25
3.3.1 Statistical Analysis of the Conditions . . . . .	26
3.3.2 Fitness . . . . .	27
3.3.3 Robustness . . . . .	27
3.3.4 Evolvability . . . . .	28
3.3.5 Structure . . . . .	29
3.4 Expected Results . . . . .	31
<b>4 Results and Discussion</b>	<b>33</b>
4.1 Results . . . . .	33
4.1.1 Control . . . . .	34
4.1.2 Mutation Up . . . . .	40
4.1.3 Mutation Down . . . . .	42
4.1.4 Selection Up . . . . .	47
4.1.5 Selection Down . . . . .	50
4.1.6 Population Up . . . . .	53
4.1.7 Population Down . . . . .	55
4.1.8 Statistics and Combined Conditions . . . . .	56
4.1.9 Genome Structure . . . . .	65
4.1.10 Evolvability . . . . .	71
4.1.11 Robustness . . . . .	73
4.2 Discussion . . . . .	75
<b>5 Conclusions and Future Work</b>	<b>79</b>
5.1 Conclusions . . . . .	79
5.2 Relation to Real-World Organisms . . . . .	80
5.3 Limitations and Future work . . . . .	81
5.3.1 Experimental Design Limitations . . . . .	81
5.3.2 Limitations of the Aevol Model . . . . .	82

# List of Figures

1.1	Unknown phylogeny . . . . .	5
2.1	Overview of Aevol’s architecture. . . . .	13
2.2	Overview of Aevol’s concept of fitness. . . . .	16
2.3	Lineage basic illustration. . . . .	18
3.1	Experimental target function . . . . .	24
4.1	Control genome size, all seeds . . . . .	34
4.2	Control condition percent non-coding . . . . .	35
4.3	Control condition fitness . . . . .	36
4.4	Control avg. size of functional genes . . . . .	37
4.5	Control gene density . . . . .	38
4.6	Control robustness . . . . .	39
4.7	Control evolvability . . . . .	39
4.8	Mutation down genome size . . . . .	40
4.9	Mutation up robustness . . . . .	41
4.10	Mutation up gene density . . . . .	41
4.11	Mutation up - percent non-coding . . . . .	42
4.12	Mutation down genome size . . . . .	43
4.13	Mutation down fitness . . . . .	44
4.14	Mutation down number of functional genes . . . . .	45
4.15	Mutation down gene density . . . . .	46
4.16	Mutation down percent non-coding . . . . .	47
4.17	Selection up genome size . . . . .	48

---

## List of Figures

4.18 Selection up number of functional genes . . . . .	49
4.19 Selection up fitness . . . . .	49
4.20 Selection up percent non-coding . . . . .	50
4.21 Selection down genome size . . . . .	51
4.22 Selection down percent non-coding . . . . .	52
4.23 Selection down number of functional genes. . . . .	52
4.24 Population up genome size . . . . .	53
4.25 Population up percent non-coding . . . . .	54
4.26 Population down genome size . . . . .	55
4.27 Population down percent non-coding . . . . .	56
4.28 Genome size . . . . .	57
4.29 Genome size - percent change . . . . .	59
4.30 Genome size - last 50k generations . . . . .	60
4.31 Fitness all seeds all conditions . . . . .	62
4.32 Mean fitness histogram . . . . .	63
4.33 Metabolic error . . . . .	64
4.34 Non-coding DNA . . . . .	66
4.35 Mean number of functional genes . . . . .	67
4.36 Mean number of non-functional genes . . . . .	68
4.37 Average size of functional genes . . . . .	70
4.38 Evolvability plot, all seed . . . . .	72
4.39 Robustness box and whisker plot . . . . .	74

# List of Tables

3.1	Table of parameters . . . . .	25
3.2	Aevol robustness statistics . . . . .	28
3.3	Aevol's stats: genes and base pairs . . . . .	30
3.4	Aevol's stats: fitness and mutation . . . . .	30
3.5	Experiment expectations . . . . .	31
4.1	Control Population Mean Fitness, Gens 0-50k, 450k-500k . .	36
4.2	Genome size - mean and std. dev. . . . .	58
4.3	Genome size rank sum statistics . . . . .	58
4.4	Genome size - last 50k generations mean & std. dev. . . .	61
4.5	Fitness means and standard deviations. . . . .	65
4.6	Non-coding DNA mean and standard deviation . . . . .	66
4.7	Number of functional genes - mean and standard deviation .	68
4.8	Number of Non-functional Genes - Mean & St. Dev. . . .	69
4.9	Mean functional gene size and standard deviation . . . . .	70
4.10	Average size of functional genes - rank sum and p-value . .	71
4.11	Evolvability - rank sum and p-value . . . . .	73
4.12	Evolvability mean and standard deviation . . . . .	73
4.13	Robustness rank sum & p-values . . . . .	74
4.14	Robustness means and standard deviations . . . . .	75
4.15	Experiment result summary . . . . .	76



# Chapter 1

## Introduction

One way of thinking about evolution is with regard to the change in frequencies of alleles (variants of genes) in a population over time. In the field of population genetics, the *Hardy-Weinberg principle* states that genetic variation (diversity of gene frequencies) in a population will remain constant from generation to generation in the absence of disturbances [9]. There are five “Hardy-Weinberg assumptions” which must hold for this to be true: no mutation, random mating, no gene flow (i.e. no transferring of genetic material from one population to another), infinite population sizes, and no selection. If any of these assumptions does not hold, then this may change the frequencies of alleles in a population, which allows evolution to occur. The mechanisms for evolution, then, are the opposite of these assumptions, namely: mutation, non-random mating, gene flow, finite populations, and natural selection. Pulling at any of these levers has an effect on the genetic variation of a population and thus impacts their genome.

Several models have been proposed to illustrate the effects on the population of violating these assumptions. The *Moran model*, named after the Australian statistician Patrick Moran, can be used on populations of finite size to model the impact of neutral drift (a mutation spreading through the population which has no impact on fitness), selection, or mutations. In the simplest version of the neutral drift model, for example, a population consists of two types, A and B, and in each generation one individual is randomly chosen to reproduce and another individual is randomly chosen to die. Given a population with  $N$  individuals and  $i$  individuals of one type

---

( $0 \leq i \leq N$ ), the transition probabilities from one state to the next (increasing, decreasing, or maintaining the number of one type) can easily be calculated. The model concludes that given enough time, however, the population reaches “*absorbing*” states in which the population is all of one type, either A or B, with a probability of  $\frac{i}{N}$  due to all organisms having equal fitness (and thus being equally likely to be selected at random). The impact of genetic drift on bacterial genome size has been investigated extensively by Kuo et al. [20] who found further evidence that “evolutionary forces that act on individual genes have profound effects on the overall architecture of bacterial genomes.”

As mentioned above, changes to the population size also causes evolution to occur. The American geneticist Michael Lynch argued in a seminal paper, “The Origins of Genome Complexity,” that it was largely due to the increase in organism size—and thus the decrease in effective population size—that genome complexity increased, both in prokaryotes (e.g. bacteria) and eukaryotes (e.g. humans). This resulted in an increase in the number of genes and the amount of non-coding DNA, which in turn provided a basis for increased complexity. He argues: “the transitions from prokaryotes to unicellular eukaryotes to multicellular eukaryotes are associated with orders-of-magnitude reductions in population size; by magnifying the power of random genetic drift, reduced population size provides a permissive environment for the proliferation of various genomic features that would otherwise be eliminated by purifying selection” [23].

By contrast, reductive evolution is the process of the average genome size of a species shrinking over time, with respect to both the number of base pairs and genes. Reductive evolution is an interesting phenomenon because it was sometimes hypothesized that increasing genome size and genomic complexity (measured, for example, via the number of genes) were closely tied to the complexity of organisms. With the advent of genomic sequencing, however, it quickly became apparent that genome size (sometimes called the “C-value”) and organismal complexity are not necessarily synchronized; this is known as the “C-value paradox.”

As an example of reductive evolution, some species of bacteria have experienced reductive evolution over the course of millions of years, and this reduction in their genome has lead to a loss of genes, certain regulatory

---

abilities, and more. It has also been theorized that reductive evolution may be responsible for the origin of eukaryotic cells, with the “symbiogenesis” theory suggesting that prokaryotic cells may have eventually become the organelles inside eukaryotic cells, with many of the prokaryotic genes being lost due to the mutualistic nature of living in the more protected environment of the cell body [35]. One free-living bacterial species which has exhibited clear tendencies towards reductive evolution is the marine cyanobacteria *Prochlorococcus*, some of whose strains have experienced a reduction of nearly 40% of their base pairs when compared to larger strains of their closest living relative, *Synechococcus*. Even among strains of *Prochlorococcus*, the difference between some of the larger and smaller strains is upwards of 38% [2]. Despite being extensively studied, the underlying mechanisms and full impact of reductive evolution are not fully understood and are an area of intense current research. Several competing explanations exist for these mechanisms, from the influence of population size, genetic drift (defined below), or selection [2], which are discussed in Chapter 2.

Previously, reductive evolution has also been studied via the methodology of comparative genomics, in which genomic features (e.g. DNA sequences, genes, gene order, etc.) were compared between organisms or species. The idea is that related organisms will have features in common which are encoded in their respective genomes, and that these features will have been conserved over the course of evolution. Often, an “alignment” of genomic sequences from two or more organisms is performed, in which the sequences are lined up so that matching positions in the sequence are correlated with each other, allowing one to see “orthologous” sequences (i.e. sequences of common ancestry). Based on these connections, evolutionary connections are inferred, based on the assumption that more closely-related genomes are more likely to be of recent common ancestry. This allows one to deduce phylogeny (evolutionary history and relatedness) of different organisms. In addition to the computational challenges presented by this approach, one of the biggest drawbacks of this methodology is that the individual steps are not easily identifiable; one may only analyze discreet moments in time (for which one has sequences), and any intermediate steps are lost to evolutionary time.

Although it would provide more conclusive evidence, performing *in vivo*

---

experiments with living organisms is often impractical because of the difficulty or impossibility of reproducing natural environmental conditions in a laboratory. Such experiments are often too costly in terms of both time and resources. As an alternative, *in silico* experimental evolution is one option that can be used to study the conditions under which an organism's genome may become reduced. In this method, organisms and their evolution over thousands or millions of generations are simulated in software. In this manner, one can control and evaluate every aspect of their evolution over time and a full record of their lineage may be maintained and studied, allowing one to go back and closely examine every step of the evolutionary period for a greater understanding of the factors that lead to specific effects on the genome. The *in silico* tool *Aevol* is one such platform which realistically models bacterial genomes and evolution, allowing one to draw conclusions about their real-world counterparts. In the following thesis, the results of experiments in artificial evolution are presented which aim to identify and evaluate several factors which potentially lead to changes in genome structure and a reduced genome in simulated bacteria using the *Aevol* platform.

Among the difficulties of studying reductive evolution with *in vivo* evolutionary experiments, one of the most difficult obstacles to overcome is the lack of a full ancestral record. This lack of a full phylogeny can make it difficult or impossible to tell exactly when and how a specific event occurred, or a trait evolved or was lost, as illustrated in Figure 1.1.

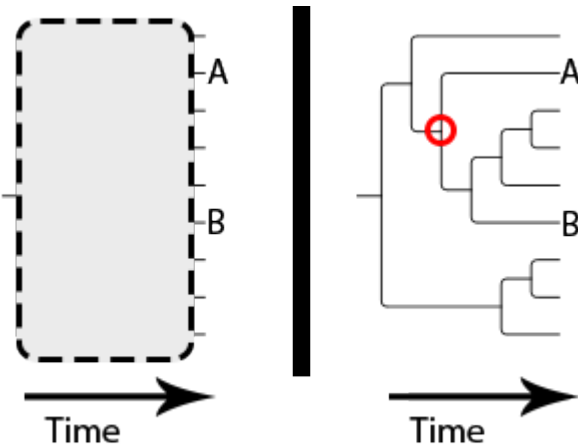


Figure 1.1: An illustration of unknown phylogeny. Since the phylogenetic information under the shaded box is typically not known, the point of divergence (red circle) can't be determined.

In this example, two related organisms A and B are compared with an attempt to determine when and how a specific trait was gained or lost by one of the organisms. This may be useful, for example, when attempting to estimate the relative importance (due to conservation over many generations) of some trait. Without the phylogenetic information (under the shaded box) it may not be possible to identify the point in their evolutionary history at which the two organisms diverged, making time estimates difficult or impossible.

Another major downside to *in vivo* evolutionary experiments is that they are slow. For example, the well-known *E. coli* Long-Term Evolution Experiment (LTEE) by Profesor Lenski at Michigan State University has been ongoing since February of 1988 and only passed generation 50,000 in 2010, 22 years later<sup>1</sup>. As an alternative to *in vivo* experiments, *in silico* evolutionary experiments are well-suited to the task of studying reductive evolution. Generations of organisms may be evolved within a very short time period, and a full "fossil record" of each lineage may be kept on disk for further analysis.

The *in silico* tool Aevol has a realistic artificial chemistry model which

---

<sup>1</sup><http://myxo.css.msu.edu/ecoli/celebrate50K.html>

---

was developed specifically to study genome structure. It contains tools to analyze the robustness, fitness, and evolvability of digital organisms over time. In this thesis, Aevol is used to perform experiments in silico evolution in order to determine the effects of several different conditions on the genome of a simulated “wild type” bacteria. The changes to the size and structure of the genome will be carefully examined in the following pages.

This chapter serves as the introduction to the thesis and the research problem being faced. In Chapter 2, some necessary background information is provided on reductive evolution, in silico evolution in general, and Aevol in particular. Chapter 3 describes the experimental setup. Chapter 4 provides the results and analysis of the experiments of this thesis, and Chapter 5 presents the conclusions drawn from this work.

# Chapter 2

## Background

In this chapter, some of the theoretical background information required for this thesis is examined. An overview of experimental evolution is given before moving on to a discussion of Aevol, the specific tool that was used in this thesis. The chapter closes examining how Aevol can be used to study reductive evolution and by discussing the current state of the literature surrounding reductive evolution.

### 2.1 Properties of Genomes

This section describes some general properties of evolutionary theory which will be required for this thesis. Some general properties about evolution were covered in Section 1 and now some more specific properties of genomes will be examined, as these will play a large role in the coming experiments.

#### 2.1.1 Evolvability

Evolvability is usually defined as the “prospective ability [of a population] to produce new mutations that can be used in adaptive evolution in the medium to long term” [6]. In other words, a system has evolvability if “mutations in it can produce heritable phenotypic variation”[38] and, critically, that this is not simply having a large amount of genetic diversity but rather *adaptive* diversity which provides some benefit.

There is, then, a link between evolvability and selection, since it is of course in an organism’s best interest to be able to adapt to new environ-

ments or situations. Evolvability should, therefore, be selected for, though it may not be obvious how, say, a random mutation which confers no immediate benefit (but which increases evolvability) may be selected for. One possibility might be the idea of “genetic hitchhiking”, in which an allele changes its frequency not because it is itself under selection but because it is near another gene which *is* under selection. Intuitively, if an “evolvability trait” arises which provides no immediate fitness benefit but which confers some benefit to offspring, eventually this trait will also increase in frequency as the fitness advantage conferred on the offspring causes them to be selected. The idea is discussed at greater length by Arenas et al. [10].

In real-world scenarios, it can be difficult to calculate evolvability for two reasons. First, evolvability can usually only be measured over evolutionary timescales. It isn’t usually possible to look at a genome and determine its evolvability, since this involves looking at its offspring and examining their fitness (or some other phenotype) in some environment. Second, the stochastic nature of mutations makes it very difficult in real-world scenarios to compare two populations, since one has to separate the noise of random mutations from the signal of evolvability [10].

### 2.1.2 Robustness and Antirobustness

Robustness is broadly defined as the ability of an organism to withstand disruptions or perturbations without affecting its phenotype. There are differing kinds of robustness, as well: one may describe robustness in terms of mutational robustness—which describes the extent to which an organism’s phenotype is not affected by stochastic mutational events—or one may speak of environmental robustness, which describes the ability of an organism to maintain its phenotype in diverse environments with little or no loss in fitness.

Also important is the idea of antirobustness, wherein an organism may actually *thrive* on such perturbations. This has been suggested as a possible method of minimizing the effects of *Muller’s ratchet*, wherein deleterious mutations accumulate in a population as a result of genetic drift[15]. A large number of initially-deleterious mutations may provide fodder for selection to fix more beneficial mutations in the population[34].

There is, then, a seeming trade-off between robustness and evolvability.

---

The more robust a system is, the less phenotypic variation is generated by random mutation events, and thus less evolvability. However, a key factor is to distinguish between genomic and phenotypic robustness; a strong phenotypic robustness promotes structural evolvability, as the likelihood that a mutation is deleterious is smaller in populations with more robust phenotypes. For a fuller discussion, see Wagner et al. [38].

### 2.1.3 Fitness

In population genetics, “fitness” can relate to either the genotype or the phenotype and denotes the contribution of an individual to the gene pool of the next generation; it is usually discussed in terms of *absolute fitness* and *relative fitness* [9]. The absolute fitness  $W$  of a genotype is the level of proportional change in the abundance of that genotype from one generation to the next. So if, for example, a genotype in generation  $t$  exists with abundance  $n(t)$ , then  $n(t+1) = W * n(t)$ .

Relative fitness, on the other hand, describes the change in genotype *frequency*, i.e. the fraction of all chromosomes in the population that carry a particular allele. For a population of size  $N$ , if a genotype’s frequency at time  $t$  is given by  $p(t) = n(t)/N(t)$ , then  $p(t+1) = \frac{w}{\bar{w}} * p(t)$ , where  $\bar{w}$  is the mean relative fitness in the population. This implies that  $\frac{w}{\bar{w}}$  is proportional to  $\frac{W}{\bar{W}}$ .

## 2.2 Reductive Evolution

Reductive evolution is the process by which organisms evolve to have a smaller average genome size than their ancestors via a pattern of gene loss [40]. This has been observed both in free-living bacteria such as *Prochlorococcus* as well as endosymbiotic bacteria living inside host cells (e.g. *Buchnera aphidicola* in aphids). Patterns consistent across most cases of reductive evolution are: a reduced GC content (impacting protein stability), gene loss, low non-coding to coding DNA ratios, and rapid sequence evolution [2]. Some of the hypothesized mechanisms behind reductive evolution include: limits imposed by the effective population size (i.e. “Muller’s ratchet”, described below), the “Black Queen Hypothesis”, and environmental adaptation.

In Muller's ratchet, organisms with smaller effective population sizes, such as *Buchnera aphidicola*, may lose genes because deleterious mutations accumulate in a population due to the smaller population size not allowing for enough variability. In the absence of recombination, these deleterious mutations become fixed in a population. The idea was originally put forth by H.J. Muller [29].

The Black Queen Hypothesis suggests that genes may be lost when some subset of the bacteria in a community is able to provide the same function as the lost genes for the benefit of the rest of the community, allowing some bacteria to lose those genes and receive the benefit from others [27].

Lastly, one other proposed hypothesis among many has been environmental adaptation. For example, many reduced strains of the marine cyanobacteria *Prochlorococcus* live in nutritionally-poor surface waters. It has been suggested that perhaps genome reduction is an adaptation which allows reduced strains to conserve precious nutrients [33, 13].

## 2.3 Experimental Evolution

As discussed in Chapter 1, in vivo experiments, although sometimes more realistic, have their own set of difficulties. Some examples of these difficulties include recreating challenging environmental conditions (e.g. simulating the open ocean in a laboratory) and identifying and/or simulating the multiple selection pressures acting on genomes in the real world [3]. These challenges add enormous difficulty and complexity to conducting proper experiments and isolating the specific factors which lead to particular outcomes.

In silico evolution simulates the evolution of organisms in software, thus allowing for far greater control and analysis of the environment and other experimental conditions. In contrast to in vivo experiments, a greater amount of control is also available with regard to the way organisms may interact, reproduce, and evolve. For example, a genome may be created completely from scratch or an existing genome may be fed into the simulation. Reproduction rates can depend on overall fitness, on relative fitness, or some other criterion.

Factors such as the mutation rates or selection pressure are then parameters for the model and may be kept constant or allowed to vary over

time. Given that these are parameters of the system, they may be tightly controlled, leading to a clearer picture of the factors influencing different outcomes. An underlying deterministic model can also allow for a reconstruction of the system from any given point, allowing one to easily create a record of events, including phylogenetic trees.

Although there are certainly limitations to using in silico evolution (see Section 5.3), overall in silico experimental evolution is a valuable tool for studying the underlying mechanisms of evolution when real-world experiments would be prohibitively time-consuming or expensive.

Many silico evolution tools have been used to test various aspects of evolution, and several formalisms exist to represent the process. In a “sequence-of-nucleotides” model, genomes are represented by a string of characters representing base pairs. Other formalisms include the “gene network model” in which genes are nodes in a connected graph, as well as the “digital organisms” model, in which software programs representing organisms fight for CPU time. Examples of the latter type include Tierra [32] and Avida [30], which were some of the first in silico evolution tools. DOSE, an ecology-conscious method of checking for heterozygosity (variation within a population) [8] is a more recent example of in silico experimental evolution. For a more comprehensive review, see [28].

## 2.4 Aevol

Aevol follows a “sequence-of-nucleotides” model [3] in which organisms are simulated with a binary genome which can either be generated at random or input as a previously-generated sequence. Aevol essentially consists of a repeated iteration of three main steps: 1) decoding the genome of these organisms to produce artificial proteins, 2) selecting the most fit individuals and 3) reproduction of these fittest individuals with possible variations (mutations, rearrangements, etc.). The sections below examine each of these steps in greater detail.

### 2.4.1 Why use Aevol

The in silico tool Aevol was developed to “study the evolution of the size and organization of bacterial genomes in various scenarios”[3]. The program has

also been expanded upon and tested in a variety of scenarios over the years (e.g. [31], [26], [25]). Some examples of experiments in which Aevol was the primary mechanism of in silico experimental evolution include: testing the predictability of evolution with high mutation rates as in viruses [4], determining whether selection is able to overcome evolution’s drive towards more complex organisms [21], examining the role of mutators in reorganizing the genome in order to overcome mutational load [34], examining the effects of population shape on levels of cooperation [25], modeling regulatory networks [36] and more.

As an in silico experimental evolution tool, Aevol embodies several of the advantages of in silico evolution in general. There is a “fossil record” of each generation, experimental conditions are tightly controlled, and experiments are easily repeatable. The encoding/decoding strategy of Aevol follows a biologically realistic model, in the sense that there are many degrees of freedom between an organism’s genome and its proteome. Many genes may encode for very simple proteins (e.g. if the genes contain the same or similar sequences), and by contrast, overlapping genes may code for complex proteomes.

In the following sections, the in silico experimental evolution tool Aevol will be examined in greater detail.

#### 2.4.2 Aevol’s Architecture

Aevol’s three main steps—decoding the genome, selection, and reproduction—are illustrated in Figure 2.1 and are discussed in greater detail in the following sections.

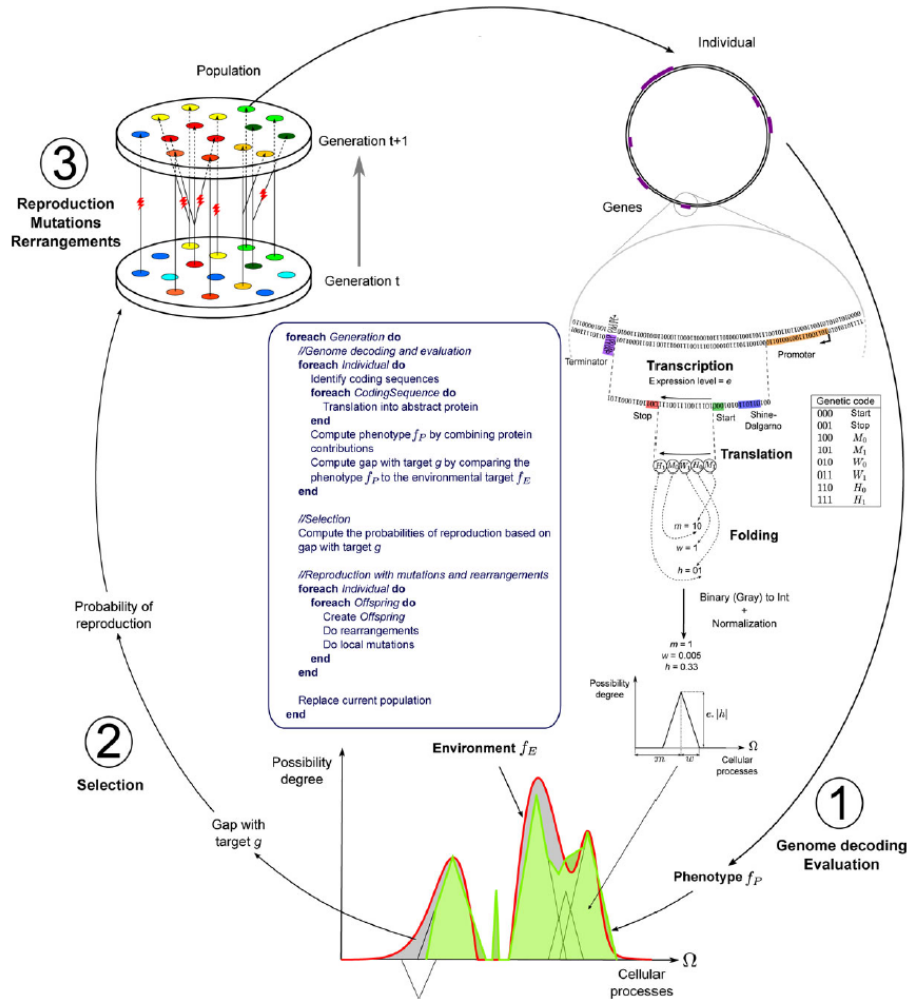


Figure 2.1: Overview of Aevol’s architecture, from [3]. In step 1, the binary genome of the organisms is decoded and the resulting phenotype (bottom, in green) is matched up against an environmental target function (red line). In step 2, the probability of reproduction is calculated for each organism, based on its fitness (gap between the environment  $f_E$  and its phenotype). In step 3, the next generation is created based on the probabilities from step 2, along with random mutations, rearrangements, etc.

### Decoding the Genome

In Aevol, a genome consists of a string of binary characters where 0 is complementary to 1. Each organism in the population has a double-stranded

circular genome which is either generated randomly or which was provided as input. To decode the genome and produce the phenotype, the sequence is searched for transcribed regions. Transcribed regions are denoted by promoter and terminator sequences. The promoter sequence is a sequence whose Hamming distance  $d$  is within  $d_{max} = 4$  mismatches of the predefined consensus sequence 0101011001110010010110. Terminators are sequences which can form a stem-loop structure with a stem size of 4 bases and a loop length of 3 bases (i.e.  $abcd***\overline{dcba}$  where  $a$  is complementary to  $\bar{a}$ ,  $b$  is complementary to  $\bar{b}$ , etc.). Lastly, the initiation and termination signals are sought, which are simply Shine-Dalgarno-like signals (i.e. 011011 \*\*\* \*000 to start and 011011 \*\*\* \*001 to stop). Lastly, an expression level  $e$  is assigned to each coding region, following the formula  $e = 1 - \frac{d}{d_{max}+1}$  where  $d$  is again the Hamming distance between the coding region and the consensus sequence given above and  $d_{max}$  is the maximum allowable distance (i.e. 4).

Once an initiation sequence is found, the following bases are read three at a time (codon by codon) until a stop codon (by default 001) is found. If a stop codon is not found, then no protein is produced. Since a transcribed region may have multiple initiation signals, operons are therefore allowed. The codons following an initiation signal encode for three parameters according to the genetic code given in Figure 2.1:  $m$  (mean),  $w$  (half-width), and  $h$  (height), which together define a triangle representing a “cellular process”.

A cellular process is simply an abstract representation of some phenotypic function and is represented by the ordered set  $\Omega = [a, b] \subset \mathbb{R}$ . Together, these cellular processes make up the organism’s proteome. To keep things simple,  $\Omega$  is a one-dimensional space in the interval  $[0, 1]$ , i.e. a “cellular process” is simply a real number, and the genomic encoding of each cellular process determines the function  $f(x) : \Omega \rightarrow [0, 1]$ . The mean  $m$  gives us the specific cellular process in the range  $[0, 1]$ . The width  $w$  describes the “scope” of the process, i.e. the *pleiotropy* of the process, meaning the subset of the protein that is in the interval  $(m - w, m + w) \subset \Omega$ . The height determines the degree of possibility of the process, i.e. its relative strength.

The codons are read one after the other and their Gray codes<sup>1</sup> are used to compute the real numbers  $m$ ,  $w$ , and  $h$  as follows. Each parameter ( $m$ ,  $w$ ,

---

<sup>1</sup>A binary encoding such that two successive values (e.g. 2, 3) only differ by at most one bit (e.g. 0011, 0010). See [11] for an overview.

$h$ ) is assigned two codons in the genetic code (see Figure 2.1), for example  $w_0 = 010$  and  $w_1 = 011$ . Any  $w_0$  codons become a 0 in the Gray code, and vice versa with 1s. So if, for example, when reading the coding sequence, the codons  $w_1$ ,  $w_0$ ,  $w_1$ ,  $w_0$  are read, the Gray code becomes 1010, which is 12 in decimal. This is done for  $m$ ,  $w$ , and  $h$ , and the resulting values are then normalized to be in the proper range.  $w$ 's range is specified in the parameter file (as `MAX_TRIANGLE_WIDTH`),  $h$  must be in the range  $[-1, +1]$  (indicating that both activating and inhibiting processes are allowed) and  $m$  must be in the range  $[0, 1]$  (the range of  $\Omega$ ).

Given the fact that there are likely multiple coding sequences in a genome, several triangles (cellular processes) are translated from the genome, each parameterized by its own  $m$ ,  $w$ , and  $h$ . These triangles form the phenotypic function  $f_P$ . *Fuzzy logic* is used to find the overall contribution of each cellular process, using the Lukasiewicz fuzzy operators<sup>2</sup>. Roughly speaking, the activating proteins are added up, as are the inhibiting proteins, and the difference between these two totals represents the final function  $f_P$ . More formally, if  $f_i$  is the possibility distribution of the  $i$ -th activator protein and  $f_j$  is the possibility distribution of the  $j$ -th inhibitor protein, then the phenotype of the individual is defined as:

$$f_P = \max \left( \min \left( \sum_i f_i(x), 1 \right) - \min \left( \sum_j f_j(x), 1 \right), 0 \right)$$

## Selection

After the genome is decoded, the organisms are tested for their fitness. Fitness in Aevol is related to the gap between the phenotype of a sequence  $f_P$  and the environmental target function  $f_E$ , as illustrated in Figure 2.1. This environmental target function  $f_E$  is a user-defined set of Gaussians which are specified in a parameter file, with each Gaussian being identified by three parameters: its height, its location along the axis, and its width. The difference between the phenotype (as calculated above) and the environmental function is the “metabolic error”, labeled  $g$  in the figure and is more formally defined as:  $g = \int_a^b f_E(x) - f_P(x) dx$ . The idea is illustrated in Figure 2.2

---

<sup>2</sup>See [https://en.wikipedia.org/wiki/Lukasiewicz\\_logic](https://en.wikipedia.org/wiki/Lukasiewicz_logic) for an introduction.

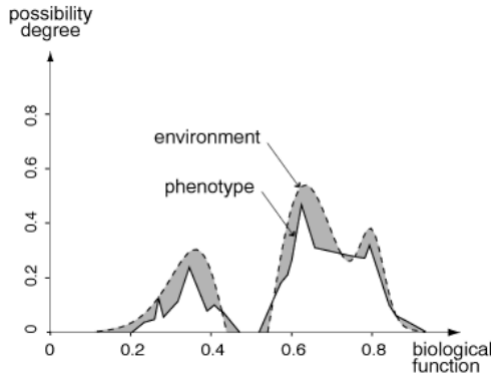


Figure 2.2: Overview of Aevol's conception of fitness, from [17]

Aevol contains several selection schemes, but here only the `fitness_proportionate` scheme will be considered, since this was the only selection scheme employed in these experiments. In this scheme, the probability of reproduction for each organism  $i$  is proportionate to its fitness, namely:

$$P(\text{reproduction}) = \frac{e^{-k*g}}{\sum_{i=1}^N e^{-k*g_i}}$$

where  $k$  is a user-definable parameter which determines the selection intensity and  $g$  is the metabolic error.

## Reproduction

Once the fittest organisms in the population are found and their probabilities of reproducing are calculated as described in the previous Section, new organisms are produced. This is done for each potential parent organism by drawing from a multinomial distribution with the probability of reproduction given above. The population size  $N$  is kept constant and a record of each generation is kept so that the phylogenetic lineages can be recreated. Since the population size is held constant, this implies that a single organism with a high probability of reproduction may produce multiple offspring and an organism with low probability of reproduction may produce none.

When new organisms are created and their genomes are copied from their parent organisms, it is at this stage that some of the driving forces in evolution occur, namely the possibility for variation through mutation, indels, and frameshifts. Offspring will receive their parents' genome but their

genome may be subject to perturbations due to stochastic effects. Mutation rates are set in the parameter file and include point mutations, insertions and deletions (indels), and rearrangements (duplication, deletions, translocations, and inversions).

The mutation, indels, rearrangement, etc. events are carried out by first determining the number  $\mu$  of such events which will occur, based on the mutation rate specified in the parameter file and drawing from a binomial distribution (e.g.  $B(L, \mu_{\text{point}})$  for point mutations,  $B(L, \mu_{\text{large deletions}})$  for large deletions, etc. where  $L$  is the size of the genome). Then a random point (or points, in the case of e.g. rearrangement) is chosen and the event is carried out, with the order of these events shuffled randomly.

## 2.5 Analyzing with Aevol

Once the experiments have completed, Aevol by default produces several statistics files which include information about genome size, the percentage of coding DNA, number of genes, average metabolic error, and many other statistics. It further includes a number of post-treatments that allow one to analyze specific individuals or the population at large, including tools for determining robustness, evolvability, coalescence, and the lineages.

One of the key features of Aevol is the ability to look back in time at the "archaeological record" of previous organisms, which is stored on disk, in order to perform various analyses. This is primarily done with a myriad of post-treatments", i.e. supplementary programs. These post-treatments generally require a `lineage` file, which is a file generated by Aevol that shows a record back in time of the line of descent for an individual. One may specify either the best-ranked individual (i.e. the fittest) or a specific individual by their unique identification number. The basic idea is illustrated below in Figure 2.3.

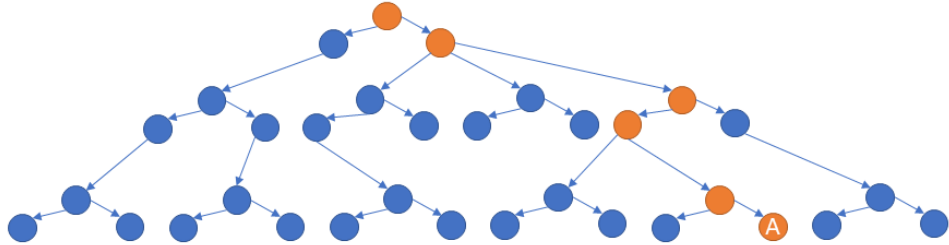


Figure 2.3: A basic illustration of a lineage. The ancestors of the individual (labeled ‘A’) can be traced back through the previous generations for all of its ancestors (all in orange).

## 2.6 Related Work

Much work has already been done in the field of reductive evolution and in silico experimentation, and this section will look at the current state of the literature.

### 2.6.1 Reductive Evolution

Regarding the influence of selection on reductive evolution, Liard et al. showed in [21] that selection for fitness is not necessarily enough to overcome the tendency of organisms to become more and more complex. They describe the existence of a “complexity ratchet,” which characterizes this tendency of organisms to increase their complexity as being irreversible once the organisms have reached a certain complexity level. In their words:

“Since gene deletion is obviously deleterious [in this scenario], the only available evolutionary path for already complex organisms is a headlong rush toward increasing complexity by acquiring new genes. Hence the ratchet clicks, further widening the fitness valley that separates the current genome from a simple one, soon making it so wide it is very unlikely to be crossed.”

Echoing the findings of Knibbe et al. [18] and performing in silico experiments with AevoL they found, however, that limiting *robustness* can overcome the tendency of organisms to become more and more complex, because this places an upper bound on the amount of information that an organism

can transmit in its genome. Limiting robustness by increasing the mutation rate forced gene elimination despite the fitness loss because it lowered the information content of the genome. A mutation rate of even  $\mu = 10^{-4}$  resulted in nearly 40% of their organisms developing a simpler genome.

Batut et al. [2] investigated many of the different hypotheses which seek to explain the mechanisms behind reductive evolution (some of which were discussed in Section 2.2), as evidenced in the marine cyanobacteria *Prochlorococcus*. Among these explanations are: limits imposed by population size and “Muller’s ratchet,” high mutation rates, the “Black Queen Hypothesis”, and environmental adaptation. Batut et al. found that generally Muller’s ratchet could explain the reduced genome size in endosymbiotic bacteria but that it was not enough to explain the reduction seen in *Prochlorococcus* due to its large effective population size—some strains of *Prochlorococcus* are estimated to have effective population sizes of up to  $10^9$ .

Regarding the “Black Queen Hypothesis,” in which members of a (bacterial) community are able to reduce their genome size because other members of a community provide the lost functionality, Batut et al. found that this hypothesis was difficult to test for but suggest it may be a useful explanation for the evolution of endosymbiotic consortia.

Given the previous discussion on high mutation rates and their impact on limiting robustness (and thus complexity), a discussion and focus on the last criterion of Batut et al., environmental adaptation, closes this section. Given the nutrient-poor environmental conditions in which *Prochlorococcus* is often found, it has been suggested that perhaps the loss of genes is adaptive, since any superfluous genes (such as those required to “respond to variation in nutrient concentrations”) inherently carry a fitness cost. However, several gene losses observed in *Prochlorococcus* suggest that the reduction was not adaptive, however. For example, many DNA repair genes were lost, and the immediate fitness benefits of such a loss are not obvious.

Regarding genome structure, in the same experiments mentioned above, Knibbe et al.[18] also found, via in silico experimentation, that the accumulation of non-coding DNA strongly depends on the mutation rate. This in turn affects the selection trade-off between reliably passing on the existing genome and having the mutational variability to adapt to new challenges. Under higher mutation rates, their organisms closely resembled

viral genomes in that they had almost no non-coding sequences. When the selection strength was larger, genomes were larger. Another aspect of genome structure, namely gene density, was examined by Kuo et al. [20], who examined the role of genetic drift on gene density (i.e. the ratio of the number of genes per number of base pairs) and found that, as the ratio of non-synonymous to synonymous substitutions increased, gene density varied much more greatly.

### 2.6.2 Investigations in Experimental Evolution

Koskineni et al. [19] performed in vivo experiments on the bacterium *Salmonella enterica* in which the effects on fitness of random deletions was measured. Some 25% of the deletions actually caused an increase in fitness under some conditions, suggesting that there is a certain cost associated with having superfluous genes and thus gene loss may be selected for under certain conditions. In the usual race between the gene-preserving force of selection and the natural tendency of bacterial genomes towards deletion and streamlining, Koskineni suggests that perhaps it is sometimes a team effort.

Liard et al. showed in their experiments with Aevol that complexity can arise in organisms in even the most simple of environments (a single triangular target function) and with the most basic beginnings (a single gene and protein) [21]. They found that the complexity continues to increase, even when the resulting organisms are much less fit than the simpler ones, and that this complexity even overcomes selection. They also found that whether an organism would develop into a simple or complex organism was usually determined quite early in its evolution, around generation 10,000. Reasoning that genome compactness is a direct driver of mutational robustness, as Knibbe et al. [18] showed, and that more robust organisms can be selected over fitter organisms under heavy mutational stress as shown by Wilke et al. [41], they wondered if robustness could select for a more simplified genome. To test this, they changed the mutation rate to be exceptionally high (up to  $\mu = 1e^{-4} * bp^{-1} * gen^{-1}$ ) and ran their simulations for another 100,000 generations, and the results confirmed their expectations: The higher the differential between the old and the new mutation rate, the larger percentage of organisms evolved a more reduced genome (up to 91%

in the case of a change from  $\mu_{\text{old}} = 1e^{-6}$  to  $\mu_{\text{new}} = 1e^{-3}$ ).

## 2.7 Summary

Connecting it all together, there is, then, a natural link between the amount of non-coding DNA, coding DNA, genome size, evolvability, robustness, and selection. As the amount of non-coding bases (and often therefore overall genome size) increases through natural mutational processes, these non-coding bases can nevertheless play a crucial role in increasing evolvability by being the fodder for new potentially beneficial mutations [18]. However, a trade-off exists because the increased *mutational load* (i.e. the increasing cost of recurrent harmful mutations, as most mutations are) also carries a fitness cost. In a population whose effective population size is too small, these deleterious mutations accumulate, a phenomenon known as Muller's ratchet [29].

# Chapter 3

## Methods

With an understanding of the basics from Chapter 2, in this chapter an overview of the contributions of this thesis and an outline of the methods used in the experiments are presented.

### 3.1 Contributions

The main contribution of this thesis is a structured examination of the effects of differing conditions towards reductive evolution in simulated bacteria, as well as how these conditions affect the genome structure of these bacteria. By only changing one variable at a time, the effects of each individual condition on these goals may be isolated from the other factors, providing a clearer picture of their individual impacts. With some insights gained into the mechanisms behind reductive evolution, it is hoped that this may be mapped onto real-world organisms such as *Prochlorococcus*.

### 3.2 Experimental Designs

To assist in determining which conditions might lead to reductive evolution, one must isolate individual variables and change just one thing at a time in order to see what effect, if any, it has on the final genome. To that end, a series of experiments were designed and conducted in which a “wild type” genome was allowed to evolve in differing conditions for 500,000 generations before analyzing the effects. To first create the wild type, a genome was gen-

---

### 3.2. Experimental Designs

erated randomly in Aevol which had at least one coding gene and which was allowed to evolve for 10 million generations in a non-varying environment. By the beginning of its use in these experiments, the wild type comprised 13,237 base pairs with 132 functional genes (i.e. genes which produce a gene product) and around 37% non-coding DNA. The wild type was generated by Guillaume Beslon—a Computer Science professor at the National Institute of Applied Science in Lyon and a developer of the Aevol platform—and provided for these thesis experiments.

In these experiments, separate clonal populations of the wild types were created, one for each condition (including one for the controls) using the Aevol command `aevol_create`. These populations were then allowed to continue to evolve in a static environment (using the Aevol command `aevol_run`) in a total of 6 different conditions: with an increased/decreased selection strength ( $k_+/k_-$ ), an increased/decreased mutation rate ( $\mu_+/\mu_-$ ), and an increased/decreased population size ( $N_+/N_-$ ).

For all experiments here, the original target environmental function in which the wild types were generated was also used. This environmental target function,  $f_E$ , is comprised of three Gaussian functions  $y(x)$ , each of which is characterized by a height  $h$ , mean  $m$ , and width  $w$ :

$$y(x) = h * e^{\left(\frac{-(x-m)^2}{2*w^2}\right)}$$

A visualization of the target function used in the experiments,  $f_E$ , can be seen below in Figure 3.1. Each Gaussian's parameters  $h$ ,  $m$ , and  $w$  are given in the figure. The gray shaded area is the phenotypic target area.

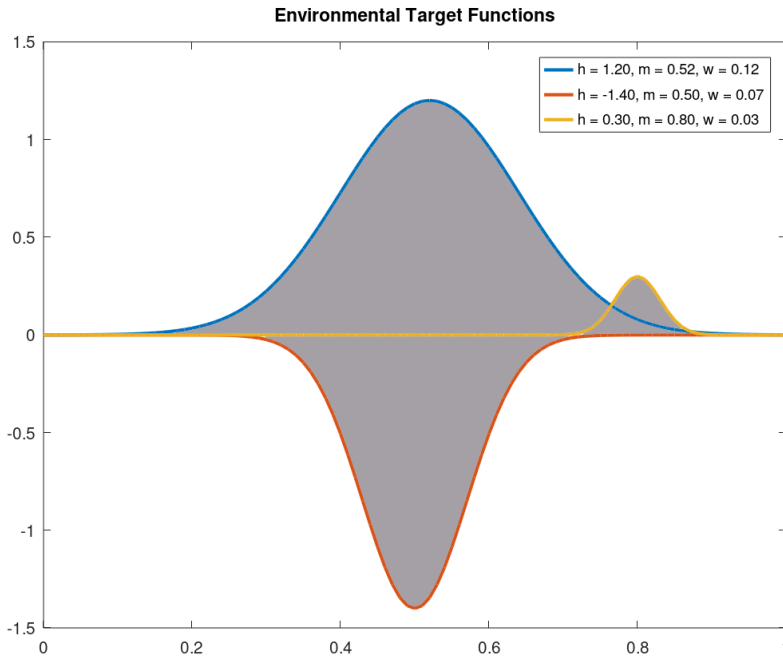


Figure 3.1: A visual representation of the target function  $f_E$  for the experiments.

In addition to the six tested changed conditions (i.e.  $\langle \mu_+/\mu_- \rangle$ ,  $\langle k_+/k_- \rangle$ , and  $\langle N_+/N_- \rangle$ ), a control condition experiment was performed in which the wild type was simply allowed to continue to evolve for the 500,000 generations with the same parameters as during the generation of the wild type. To minimize bias, for each condition five runs were performed (that is, 5 rounds of  $\mu_+$ , 5 rounds of  $\mu_-$ , etc.), where each run had a differing random seed to control for the deterministic effects of the pseudorandom nature of Aevol's stochastic processes. This lead to a total of 35 experiments, all of which were carried out on a cluster from bwCloud<sup>1</sup>.

The resulting data was processed using a combination of Python<sup>2</sup>, Pandas<sup>3</sup>, and Jupyter Notebooks<sup>4</sup>.

<sup>1</sup><https://www.bw-cloud.org/>

<sup>2</sup><https://www.python.org/>

<sup>3</sup><https://pandas.pydata.org/>

<sup>4</sup><https://jupyter.org/>

### 3.2.1 Inputs

In Table 3.1, the parameter values for all input parameters for Aevol may be found. Please note that for  $\mu$ , this represents the mutation rates for point mutations, small insertions, and small deletions. The rearrangement rates were not changed under any condition and were always  $1e - 6$  for duplications, deletions, translocations, and inversions.

<b>Condition</b>	<b>Parameter</b>		
	$\mu$	$k$	$N$
control	$1.00E-7$	1000	1024
mutation up ( $\mu_+$ )	$4.00E-7$	1000	1024
mutation down ( $\mu_-$ )	$2.50E-8$	1000	1024
selection up ( $k_+$ )	$1.00E-7$	4000	1024
selection down ( $k_-$ )	$1.00E-7$	250	1024
population up ( $N_+$ )	$1.00E-7$	1000	4096
population down ( $N_-$ )	$1.00E-7$	1000	256

Table 3.1: Table of input parameters.  $\mu$  is the mutation rate,  $k$  is the selection strength, and  $N$  is the population size.

As can be seen in Table 3.1, only one parameter varied per condition in order to isolate potential influences on the outcome. A multiplier of 4 was chosen for the differing conditions relative to the control condition (e.g.  $|N_+| = 4096 = 4 * |N_{\text{control}}| = 4 * 1024$  organisms). This choice of a 4x multiplier was chosen following the model of Carde et al.[7]. The goal of their experiments was to use Aevol as a pedagogical tool, teaching a high school student (Carde) to use the scientific method to investigate “how to reduce a genome.” The methodology of this thesis is similar to their strategy, namely by providing both an increased and decreased condition for each criteria and otherwise keeping parameters and environments static.

## 3.3 Evaluation Strategy

In this section, the criteria to be used for evaluating the results are examined. The primary criteria will be calculating the evolved genome’s evolvability, robustness, and structure, with a statistical analysis of the changed

conditions vs. the control condition.

### 3.3.1 Statistical Analysis of the Conditions

First, it must be determined whether the results of the condition (e.g. mutation up, selection down, etc.) were significantly different from the control condition, statistically speaking. To do this, for some test (e.g. robustness, evolvability, etc.) the mean across all seeds is calculated for a condition (e.g.  $\mu_+$ ) and compared to the mean across all seeds of the control condition. For these types of comparison, the “Mann-Whitney U” test is used. The Mann-Whitney U test is similar to the Wilcoxon signed-rank test but it is used when the distribution of the two samples cannot be assumed to be normally distributed. The Mann-Whitney U test can also be used when the sample sizes are different, for example when the number of base pairs is different between two organisms.

The purpose of the Mann-Whitney U test is to check whether two independent samples were selected from populations having the same distribution. Similar to other rank-sum tests, the test consists of the following steps:

1. Assign numeric ranks to all observations;
2. Add up the ranks for the observations from the first sample, giving us  $R_1$
3. The statistic  $U_1$  for the first sample is given by:

$$U_1 = R_1 - \frac{n_1 * (n_1 + 1)}{2}$$

where  $n_1$  is the sample size for the first sample and  $R_1$  is the sum of the ranks from the first sample.

The  $U$  statistic for the second sample (i.e.  $U_2$ ) is computed analogously. Then the final statistic  $U$  is given by  $U = U_1 + U_2$  which, for sample sizes greater than 20, is approximately normally distributed. Then the standard score is given by:

$$z = \frac{U - m_U}{\sigma_U}$$

### 3.3. Evaluation Strategy

where  $m_U$  and  $\sigma_U$  are the mean and standard deviation of  $U$ .

$$m_U = \frac{n_1 * n_2}{2} \text{ and } \sigma_U = \sqrt{\frac{n_1 * n_2 (n_1 + n_2 + 1)}{12}}$$

In these experiments, the Python library function `scipy.stats.mannwhitneyu` was used on Pandas DataFrames containing the observations in order to calculate the Mann-Whitney U statistic. This function also calculates the p-value. With the typical confidence level of  $\alpha = 0.05$ , if the p-value is below 0.05, the null hypothesis  $H_o$  must be rejected that the two samples (i.e. the control and the condition) are from the same distribution; otherwise it must be accepted.

#### **3.3.2 Fitness**

Fitness in Aevol is closely tied in to the “metabolic error”. This error,  $g$ , is calculated as the gap between the environmental function  $f_E$  and the phenotype of the organism,  $f_P$ . Once  $g$  is determined as described above in Section 2.4.2, it may be used to calculate the actual fitness of the organism according to the equation:

$$\text{fitness} = \exp(-k * g)$$

where  $k$  is the *selection coefficient* variable set by the user in a parameter file. Aevol provides fitness statistics both for the fittest individual and for the population at large.

#### **3.3.3 Robustness**

Aevol calculates statistics for both mutational robustness as well as antirobustness. Robustness in Aevol is calculated similarly to evolvability (see Section 3.3.4): a `lineage` file (see Section 2.5) for an individual is fed to the post-treatment `misc_ancestor_robustness`, which generates a user-specified large number of offspring whose fitness is then measured. The percentage of these offspring which are neutral (i.e. whose phenotype is not affected by the mutations) is the robustness, and the percentage of positive offspring (i.e. those whose fitness is greater than their parent’s) determines the antirobustness.

### 3.3. Evaluation Strategy

In these experiments, at the end of the run of 500,000 generations a lineage file for the best individual at generation 500,000, i.e. the individual whose metabolic error was smallest, is generated. This lineage file is then fed in to the post-treatment `aevol_misc_ancestor_robustness` and robustness statistics are generated for each generation in the lineage file. The statistics produced by this post-treatment are summarized in Table 3.2 below.

<b>Robustness Statistic</b>
Fraction of positive offspring
Fraction of neutral offspring (aka reproductive robustness)
Fraction of neutral mutants (aka mutational robustness)
Fraction of negative offspring
Cumulative delta-gaps of positive offspring
Cumulative delta-gaps of negative offspring
Delta-gap for the best offspring
Delta-gap for the worst offspring
Cumulative delta-fitness of positive offspring
Cumulative delta-fitness of negative offspring
Delta-fitness for the best offspring
Delta-fitness for the worst offspring

Table 3.2: Table of robustness statistics calculated by Aevol’s `aevol_misc_ancestor_robustness` post-treatment for a provided lineage.

These statistics for both the control and the specific desired condition (e.g. mutation up) may then be compared. Because this data is somewhat noisy (owing to the fact that the fitness may change rapidly from generation to generation), box and whisker plots will be used to show the overall spread rather than plotting the robustness generation by generation.

#### **3.3.4 Evolvability**

In Aevol, evolvability is calculated by generating a large set of offspring for a specific individual (one whose lineage was generated using the post-treatment `aevol_misc_lineage`) at regular periods along their lineage and then determining the number of “positive offspring”. Positive offspring are

### 3.3. Evaluation Strategy

defined as those whose fitness is greater than their parent’s. The evolvability of an individual is then the sum total of all improvement of all of the beneficial offspring, i.e.:

$$\text{evolvability} = \frac{|\text{positive offspring of } i|}{|\text{total offspring of } i|} * \sum \Delta_{\text{fitness}}^{\text{positive offspring}}$$

where  $\sum \Delta_{\text{fitness}}^{\text{positive offspring}}$  is the cumulative sum of the fitness increase for the positive offspring. Thus, evolvability in Aevol accounts for both the likelihood of a positive mutation and the average improvement provided by said mutation. Practically speaking, to find an organisms evolvability in Aevol one must give the post-treatment `misc_ancestor_robustness` a lineage file and then multiply the fraction of the number of positive offspring (column 2) by the cumulative total of the fitness gap  $g$  of the positive offspring (column 10).

#### **3.3.5 Structure**

Another strength of Aevol is its ability to analyze changes in the structure of DNA and RNA. As with fitness, Aevol produces statistics about individuals and the population at large for many aspects of genome structure, including: the number of coding vs. non-coding bases (i.e. they respectively do or do not code for at least one protein), the average size of coding and non-coding DNAs, the number of genes, the number of “essential” base pairs (i.e. those that are part of a functional coding sequence), etc. Tables 3.3 and Table 3.4 summarize the different statistics and where they are to be found Aevol’s output files.

### 3.3. Evaluation Strategy

---

Stat File	
stat_genes_{best/glob}	stat_bp_{best/glob}
number of coding RNAs	number of bp not in any CDS
number of non-coding RNAs	number of bp not included in any functional CDS
average size of coding RNAs	number of bp not included in any non-functional CDS
average size of non-coding RNAs	number of bp not included in any RNA
number of functional genes	number of bp not included in any coding RNA
number of non-functional genes	number of bp not included in any non-coding RNA
average size of functional genes	number of non-essential bp
average size of non-functional genes	number of non-essential bp including non-functional genes

Table 3.3: Statistics found in `stat_genes` and `stat_bp` output files from Aevol. {best/glob} indicates that statistics are available for both the best individual and the average across the whole population.

“Essential” base pairs are those whose mutation would change the phenotype of the organism.

Stat File	
stat_fitness_{best/glob}	stat_mutation_{best/glob}
population size	number of local mutations
fitness	number of chromosomal rearrangements
genome size	number of switches
metabolic error	number of indels
parent’s metabolic error	number of duplications
metabolic fitness	number of deletions
secretion error	number of translocations
parent’s secretion error	number of inversions
secretion fitness	
amount of compound present in grid-cell	

Table 3.4: Statistics found in `stat_fitness` and `stat_mutation` files from Aevol. {best/glob} indicates that statistics are available for both the best individual and the average across the whole population.

### 3.4 Expected Results

Table 3.5 gives the expected behavior for each of the six conditions investigated in this thesis based on the literature review from Section 2.6. A ‘+’ indicates that an increase is expected in that area (e.g. genome size) and a ‘-’ indicates an expected decrease.

Experiment Predictions						
Effect on:	Condition					
	$\mu_+$	$\mu_-$	$k_+$	$k_-$	$N_+$	$N_-$
Genome Size	-[5, 7, 24]	+[5, 7, 12]	+[3]	-[3]	-[2, 7]	+[2, 7]
Fitness	+[1, 37]	-[37]	+[2]	-[2]	+[9, 37]	-[9, 37]
Amount of non-coding DNA	-[18]	+[18]	+[3, 18]	-[3, 18]	-[3]	+[3]
Number of genes	-[18]	+[18]	+[18]	-[18]	-[2]	+[2]
Average size of genes	-[21]	+[21]	-[3]	+[3]	-[2]	+[2]
Robustness	-[18]	+[18]	-[3, 18]	+[3, 18]	-[14]	+[14]
Evolvability	+[18]	-[18]	+[3]	-[3]	-[39]	+[39]

Table 3.5: Predictions for the experiments.  $\mu$  is the mutation rate,  $k$  is the selection rate, and  $N$  is the population size.  $\mu_+$  indicates an increased mutation rate,  $\mu_-$  a decreased rate, etc. A + in the main grid space indicates an expected increase (over the control condition) for that condition, and a – indicates an expected decrease for that condition.

As summarized in the table, a reduction in genome size is expected to occur in the  $\mu_+$ ,  $k_-$ , and  $N_+$  conditions. Based on the work of Bradwell et al., Carde et al., and Marais et al. [5, 7, 24], it is expected that an increased mutation rate (i.e. the  $\mu_+$  condition) should cause many deleterious mutations which in turn will be removed by purifying selection. Likewise, with weaker selection, the work of Batut et al. [3] indicates that with a decreased selection pressure (corresponding to the  $k_-$  condition here), many functional genes are lost, causing the organisms to be less fit on average. More interestingly, however, the reduced selection pressure is also expected to cause a loss in non-coding bases, which was the primary source of genome reduction in their experiments. This follows from the fact that, as found in a previous study by Knibbe et al. [18], the most successful genomes tend to

### 3.4. Expected Results

---

be those that produce “a little more than one ‘neutral offspring’, that is to say, offspring without mutations or with only neutral mutations” [3]. More formally, Knibbe et al. found that successful genomes fulfill  $F_v * W \approx 1$ , where  $W = \frac{e^{-k*g}}{\sum_{i=1}^N e^{-k*g}}$  is the expected number of offspring ( $k$  is the selection coefficient and  $g$  is the gap described in Section 2.4.2) and  $F_v$  is the probability of an offspring having either no mutations or only neutral ones. In other words, with reduced selection,  $F_v$  is increased because non-coding DNA is mutagenic for the surrounding genes, so a certain level of mutational variability is still selected for. Lastly, based on the work in another publication by Batut et al. [2], an increase in population size (corresponding to the  $N_+$  condition) is expected to cause a decrease in genome size, most likely because of the increased efficacy of selection in larger populations.

# Chapter 4

## Results and Discussion

This chapter presents the results of the experiments as performed according to the plan described in Chapter 3. Section 4.1 provides the data and discussion for the individual conditions and the results are discussed in more detail in Section 4.2.

### 4.1 Results

In this section, the results of the experiments are presented. For each tested condition (e.g.  $\mu_+$ ,  $N_-$ , etc.), both a graphical representation of the data and some of the statistics are given. It should be noted that in many of the figures throughout this chapter, a rolling window of the mean (either of the control or non-control conditions) or of the individual seeds was used to smooth the plots, resulting in many of the plots only showing data starting after a certain number of generations (usually 10,000). This is simply an artifact of the graphing process, and simulations were indeed carried out for 500,000 generations. Lastly, although Aevol provides statistics for both the best individual at a particular generation as well as for the population at large, since this thesis is primarily concerned with general trends, the values given in the tables and graphs are for the population at large unless specified as being for the best individual.

### 4.1.1 Control

The results of the control condition are presented first to provide a baseline for the remaining conditions. As mentioned in Chapter 3, five runs (seeds) of the experiment were performed. Beginning with genome size, the primary focus on this thesis, Figure 4.1 shows the mean number of base pairs (bp) for the population at large of the individual seeds (various colors) and the average across all five seeds (black, dashed line) for 500,000 generations.

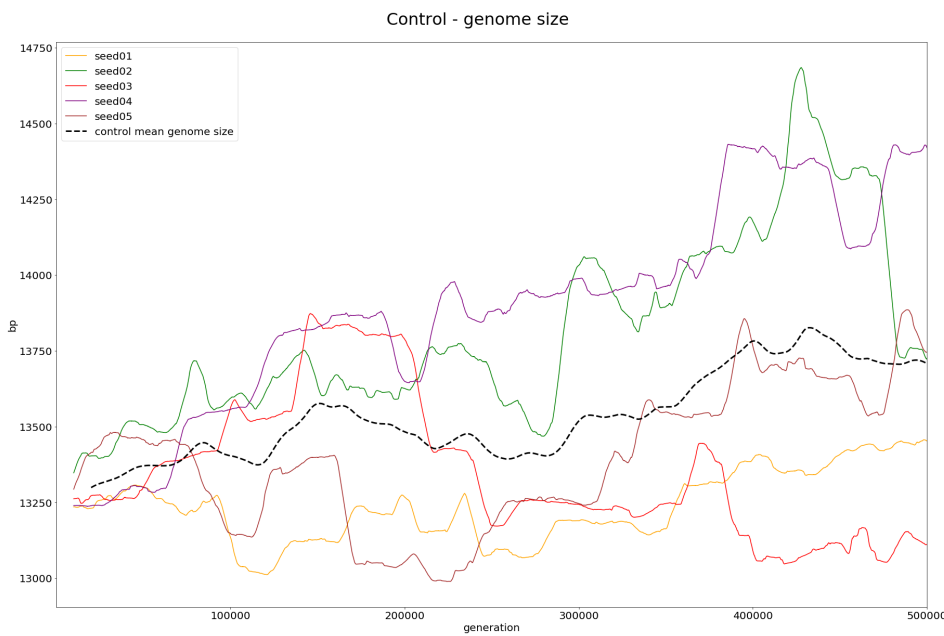


Figure 4.1: Genome size of the control condition, generations 1-500,000. The individual seeds are shown in various colors and the mean across all seeds is shown in the dashed black line.

Examining the figure, over the course of 500,000 generations the mean genome size in the control condition tended towards *gaining* base pairs, averaging just under approximately 500 new base pairs across all seeds. As can be seen in Figure 4.2, the averaging out to a modest gain in overall genome size was partially the result of the accumulation of non-coding bases.

## 4.1. Results

---

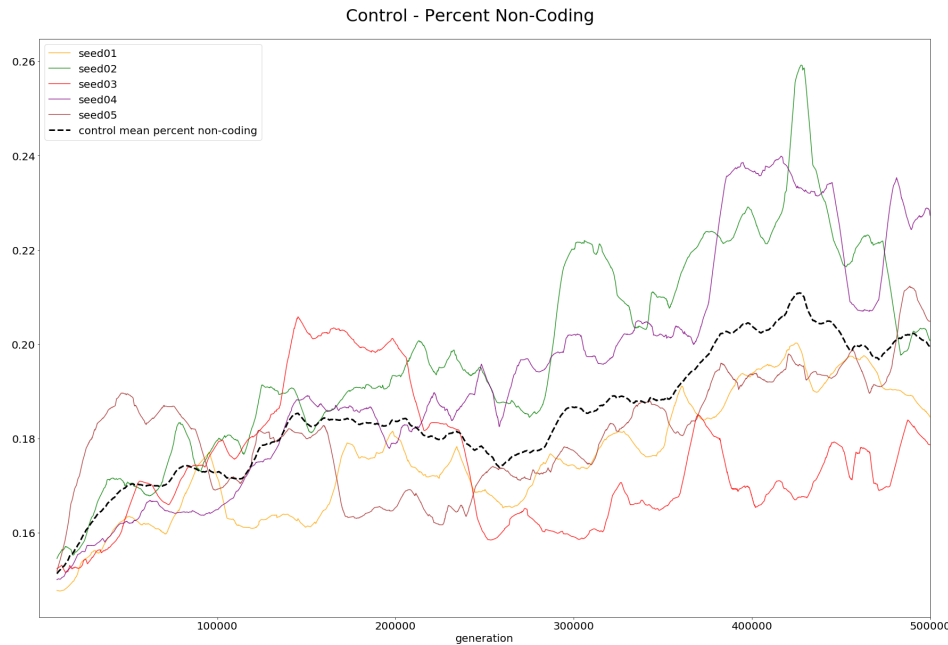


Figure 4.2: Percent non-coding for the control condition, generation 1-500,000.

Despite the slight increase in non-coding bases, however, overall population fitness continued to improve even though the wild types had already evolved for 500,000 generations in the same environment, as seen in Figure 4.3.

## 4.1. Results

---

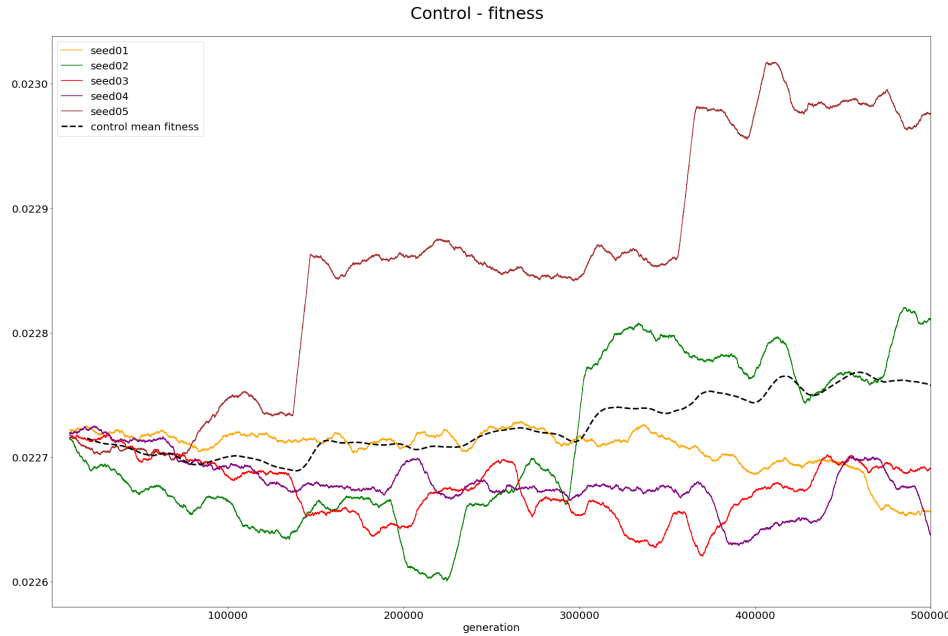


Figure 4.3: Control condition fitness, seeds and mean, generations 1-500,000. The five seeds are in various colors and the mean of these seeds is shown in black, dashed.

Table 4.1 below illustrates, however, that although the largest individual fitness improvement in a seed (seed05) was closer to 1.322%, the improvement in the all-seed mean from the first 50,000 generations to the last 50,000 generations was only 0.2333%, a very modest increase.

Control Mean Fitness, All Seeds		
fitness @0-50k	fitness @450k-500k	Percent Change
0.022709775696292796	0.02276276339318254	0.2333%

Table 4.1: Table showing the mean population fitness change from generations 0-50k and 450-500k for all seeds.

Figure 4.4 shows the change in the average size of functional genes observed in the control condition for all seeds for all 500,000 generations.

## 4.1. Results

---

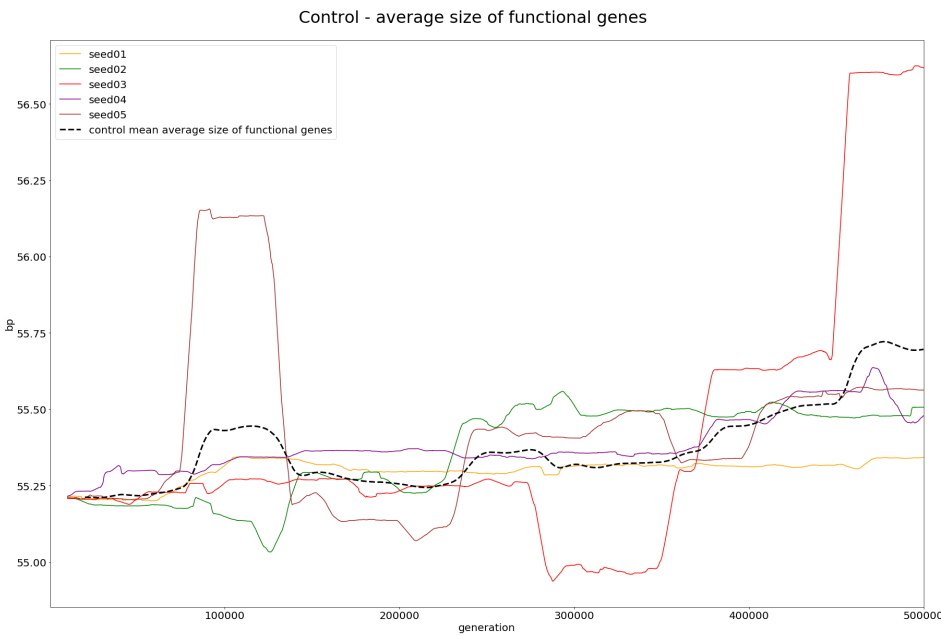


Figure 4.4: Figure showing the population mean size of the functional genes in the control condition, generations 1-500,000.

Figure 4.5 shows gene density (the number of genes per total number of base pairs). Though this is usually given per million base pairs (Mb), here it is simply the straight number of genes divided by the genome size, and is given as a convenient measure for comparison which takes into account both the number of genes and the genome size.

## 4.1. Results

---

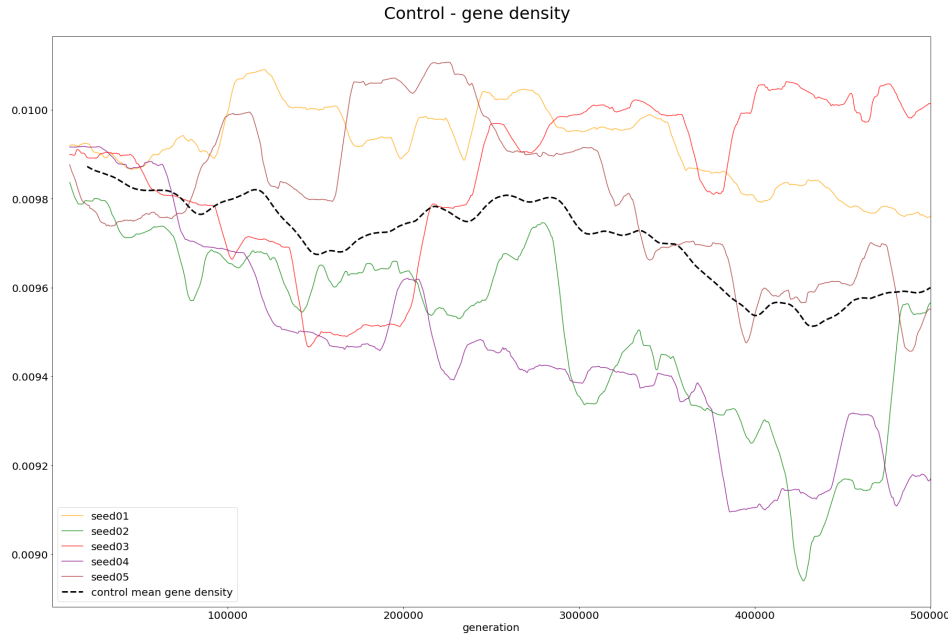


Figure 4.5: Control condition gene density, generations 1 to 500,000, all seeds

Figures 4.6 and Figure 4.7 show the control condition's robustness and evolvability, respectively. As a reminder, in Aevol, mutational robustness is calculated by finding the fraction of neutral offspring of an individual. In these figures, both robustness and evolvability are calculated based on the best individual at generation 500,000. Please note the scale of Figure 4.7, which is  $1 * e^{-8}$ .

## 4.1. Results

---

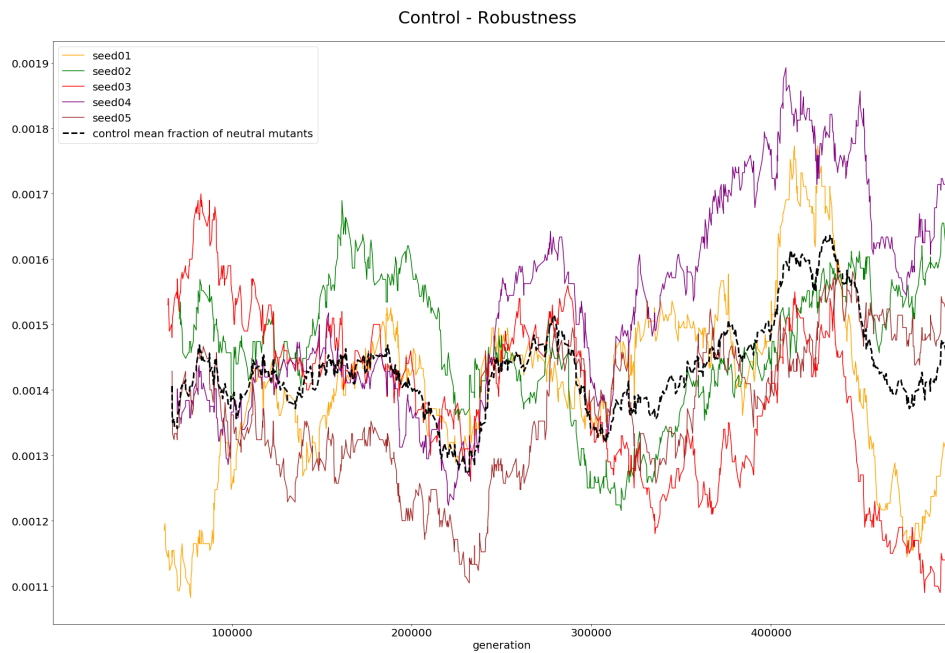


Figure 4.6: Control robustness for generations 1-500,000, all seeds.

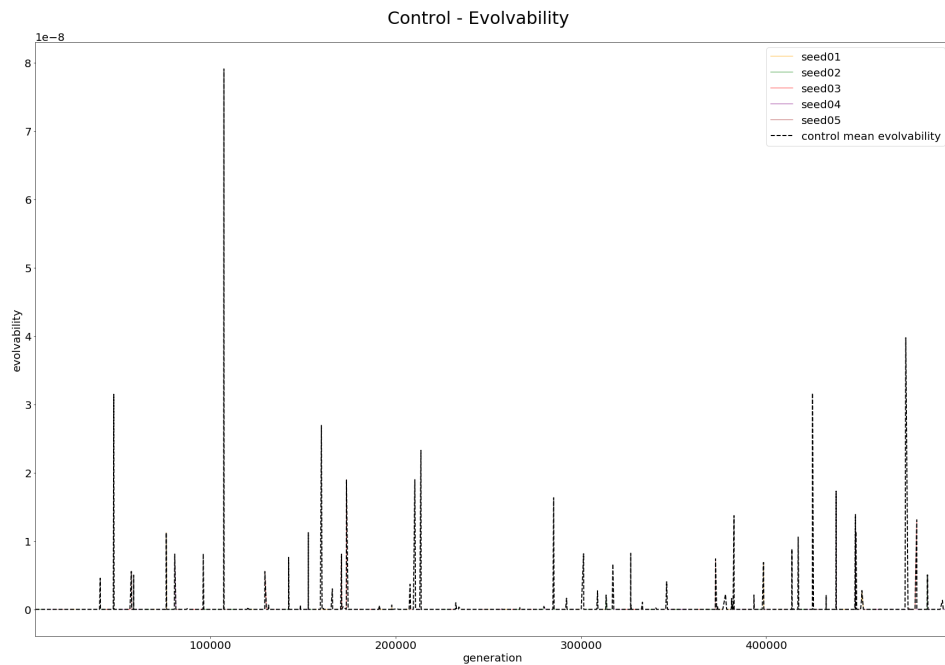


Figure 4.7: Control evolvability, all seeds.

## 4.1. Results

---

Because the wild types began these experiments having evolved for 10 million generations in a static environment, their variability was low and the genome was relatively compact (thanks to the natural streamlining effects of bacterial genomes), and thus their mutational robustness was also low.

### 4.1.2 Mutation Up

The genome size for the  $\mu_+$  condition is shown in Figure 4.8. The  $\mu_+$  population mean genome size fluctuated between being above and below the control condition, and Table 4.2 (pg. 58) makes it clear that, when considered over the whole run of 500,000 generations, the increased mutation rate lead to a slightly *larger* mean genome size (0.157661%).

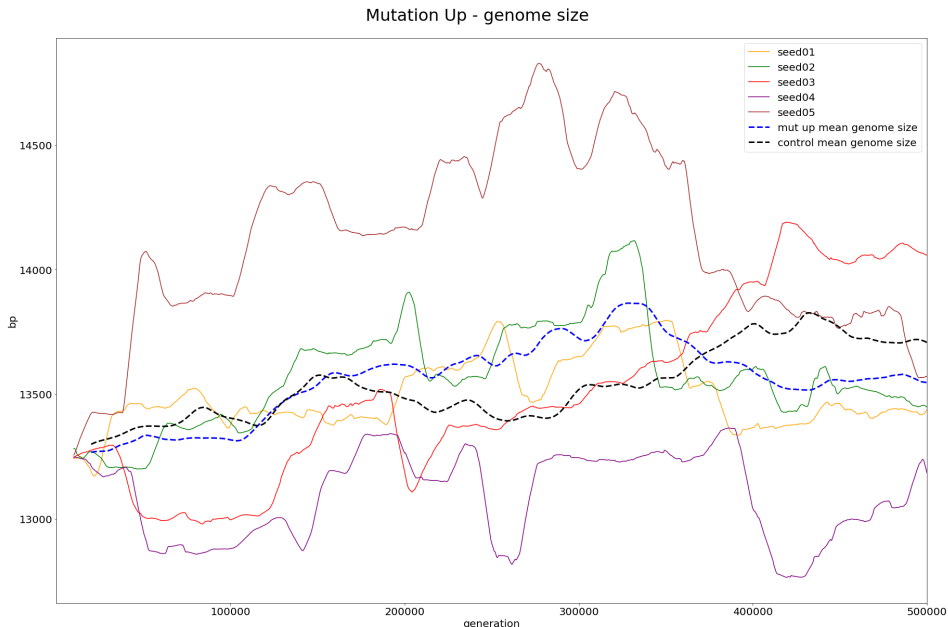


Figure 4.8:  $\mu_+$  population genome size, generations 1-500,000.

## 4.1. Results

---

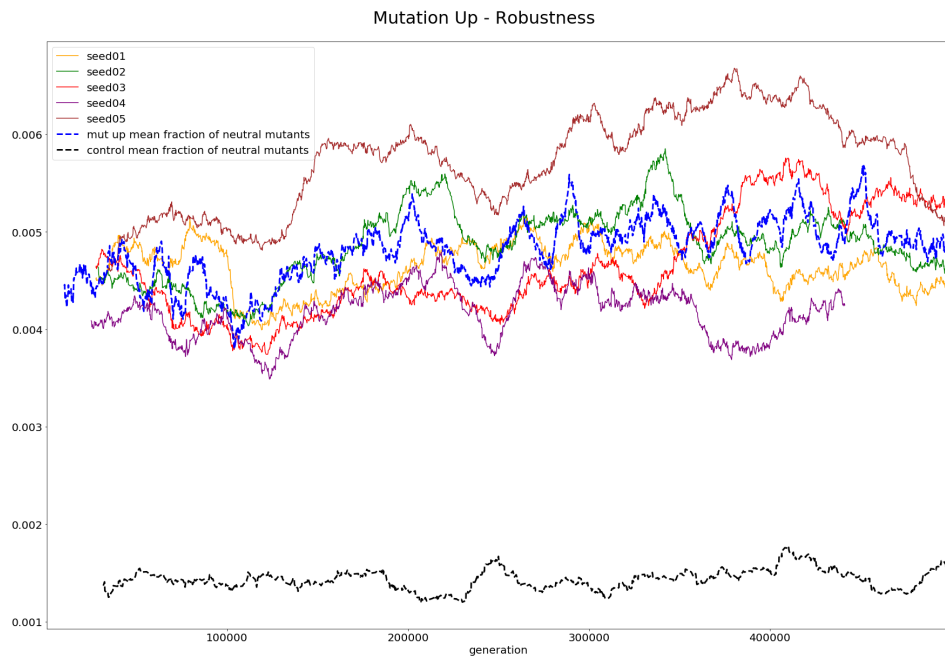


Figure 4.9: Mutation up robustness, generations 1-500,000.

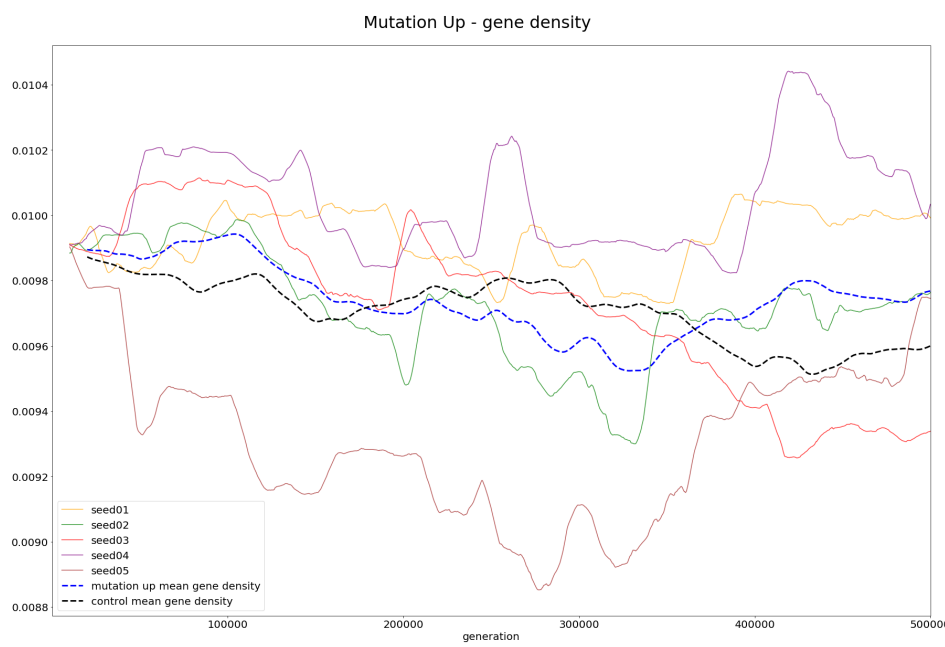
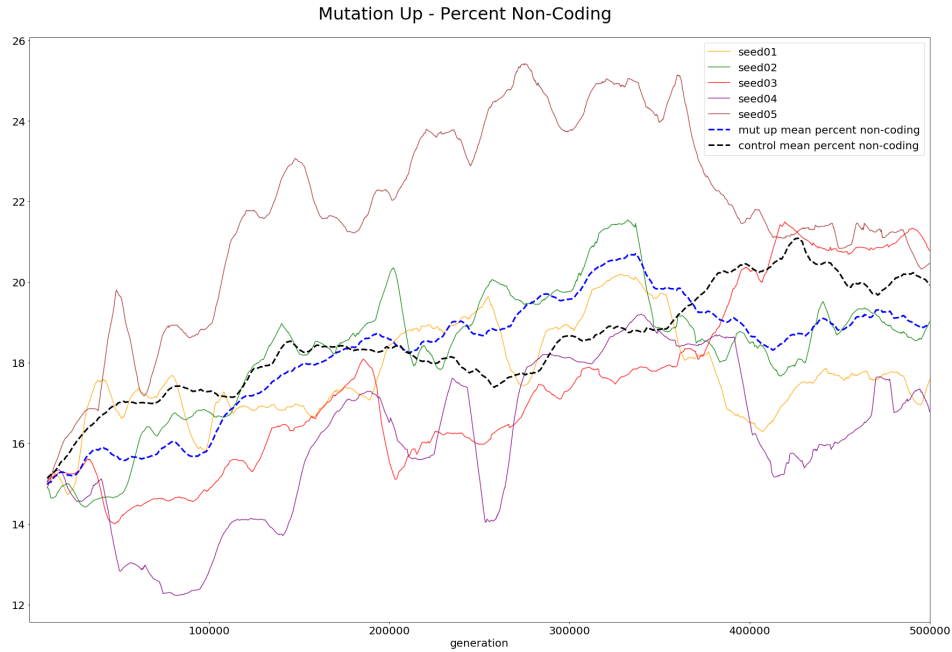


Figure 4.10: Mutation up gene density for generations 1-500,000, all seeds.


 Figure 4.11:  $\mu_+$  percent non-coding

### 4.1.3 Mutation Down

The results of decreasing the mutation rate to  $2.5e - 8$  from the usual  $1e - 7$  also had the unexpected result (according to the predictions from Section 3.4) that the genome size decreased over the control condition, though it still did not end up being lower than at generation 1. Figure 4.12 shows the data for the genome size of the  $\mu_-$  condition.

## 4.1. Results

---

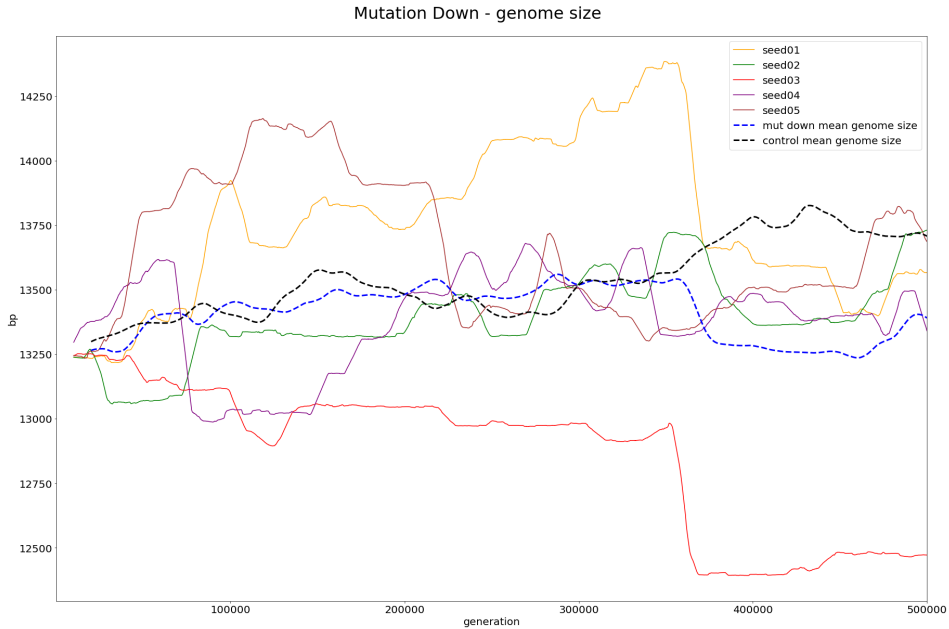


Figure 4.12:  $\mu_-$  genome size, generations 1-500,000.

The well-accepted “Drake’s rule” states that genome size is inversely proportional to mutation rate [12]. Given the reduced mutation rate of the  $\mu_-$  condition, it is expected then that the genome size should increase over the control condition, but this was not the case in these experiments.

Examining the fitness data in Figure 4.13 it is clear that overall fitness was also not negatively impacted, as one should expect given the lower likelihood of introducing deleterious mutations.

## 4.1. Results

---

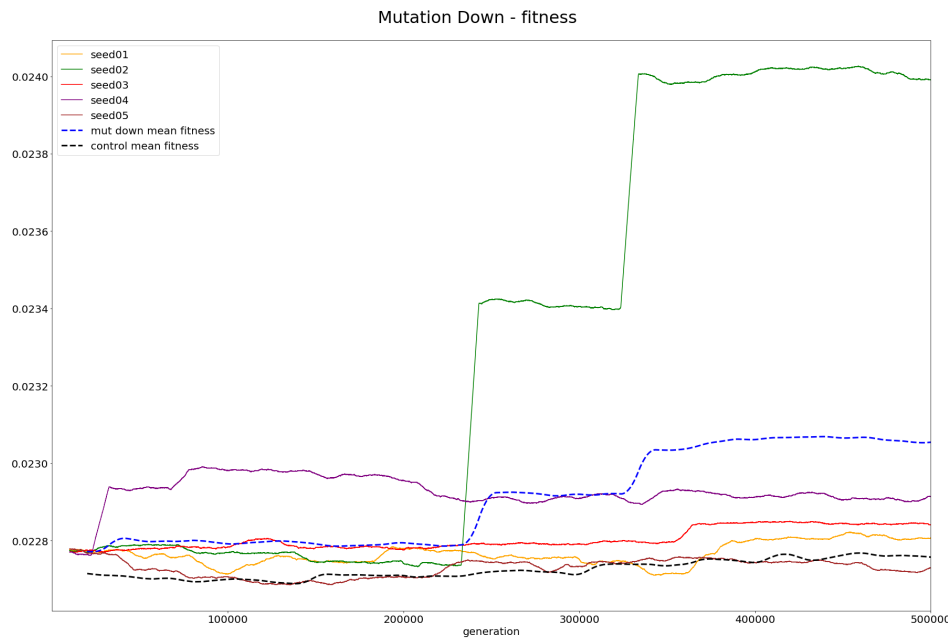


Figure 4.13: Mutation down population mean fitness, generations 1-500,000, all seeds.

Figure 4.15 shows that gene density significantly increased in the  $\mu_-$  condition somewhere around generation 360,000, and this also corresponds to a big bump in fitness, as shown in Figure 4.13 above.

## 4.1. Results

---

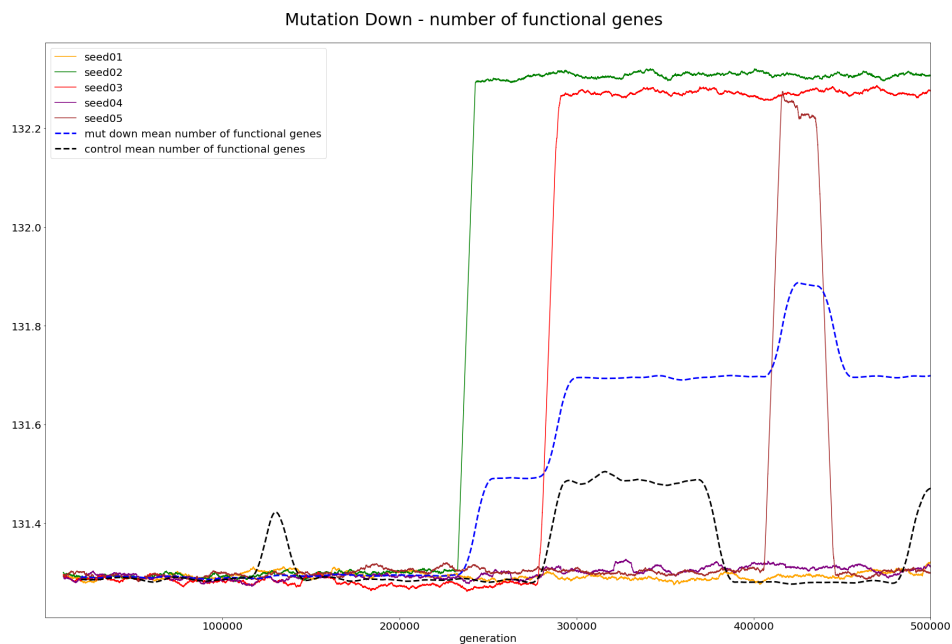


Figure 4.14: Mutation down - population mean number of functional genes, generations 1-500,000, all seeds

## 4.1. Results

---

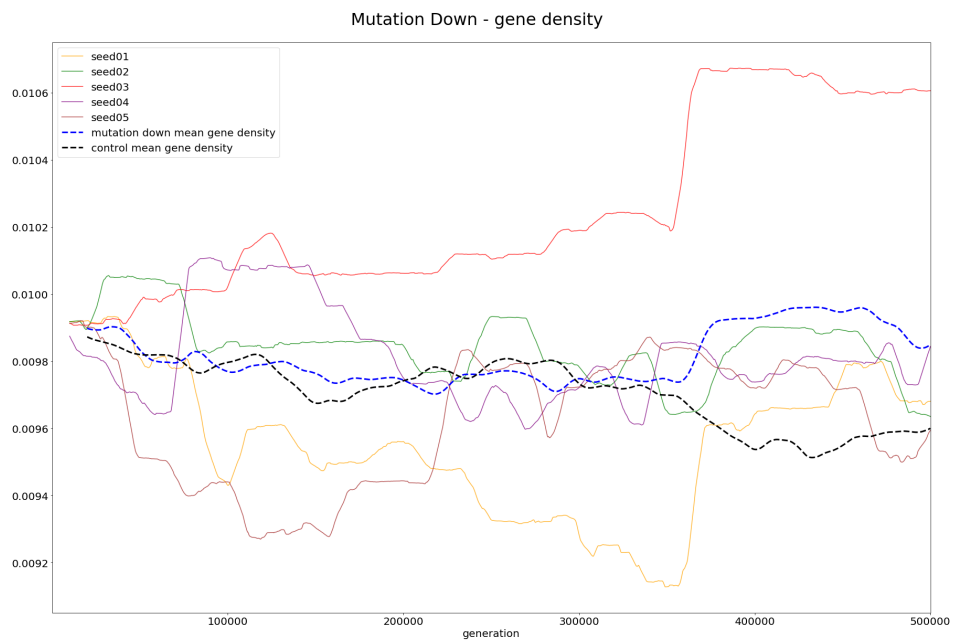


Figure 4.15:  $\mu_-$  population mean gene density, generations 1-500,000, all seeds.

## 4.1. Results

---

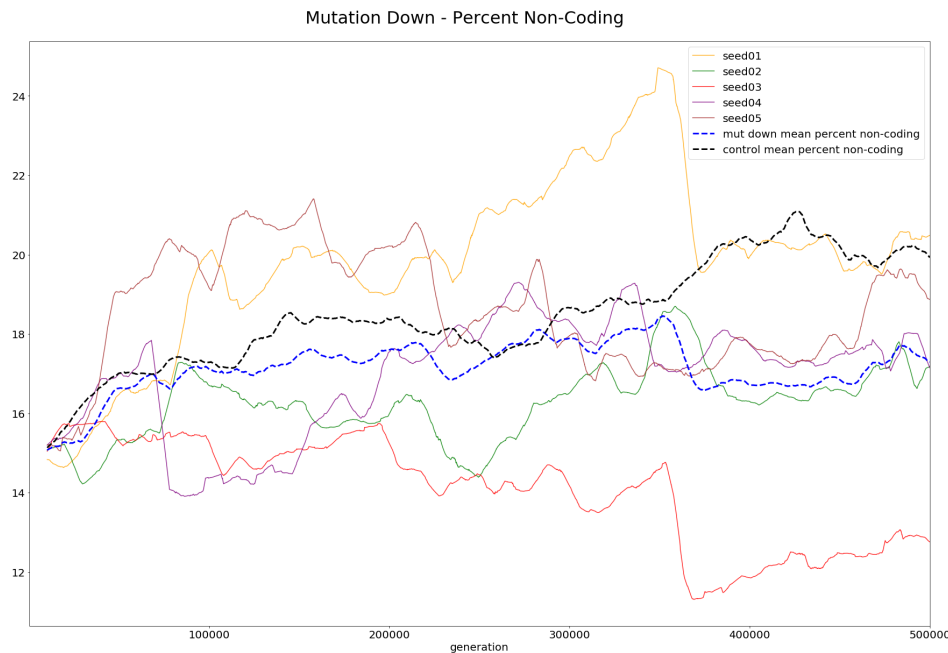


Figure 4.16:  $\mu_-$  population mean percent non-coding, generations 1-500,000, all seeds.

### 4.1.4 Selection Up

Figure 4.17 shows that the genome size increased under increased selection, confirming the expected results based on Batut et al. [3].

## 4.1. Results

---

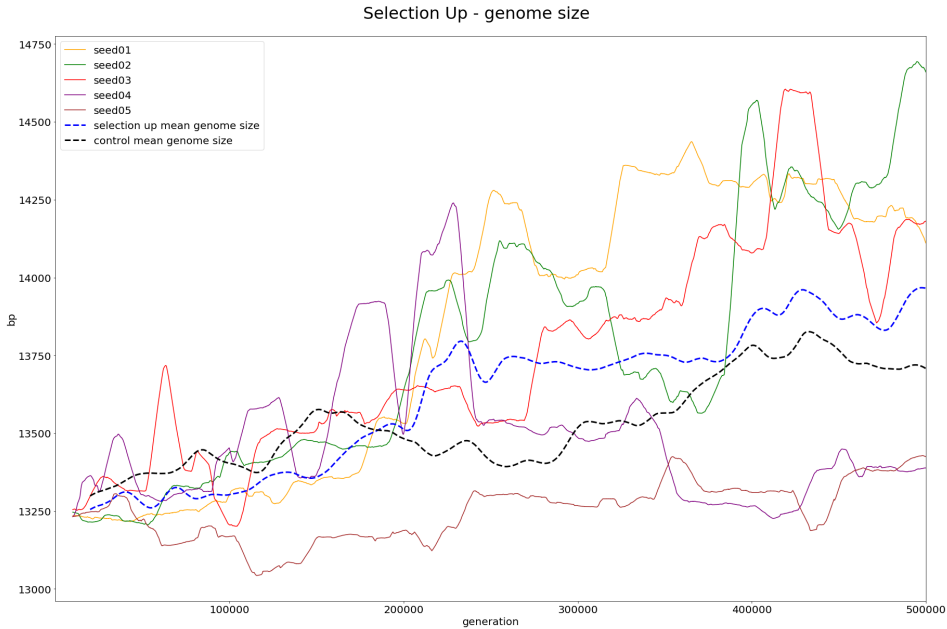


Figure 4.17:  $k_+$  genome size, generations 1-500,000.

As with the experiments of Batut et al., the primary gain seems to be in the number of genes, as Figure 4.18 illustrates. Figure 4.19 shows that fitness overall saw an upward trend, also confirming the results of Batut et al. The large disparity in the fitness scale between the  $k_+$  and the control conditions is due to Aevol’s `fitness_proportionate` selection method. Recall that in the `fitness_proportionate` selection method, the probability  $p$  of reproduction for an organism with gap  $g$  is given by:

$$p = \frac{e^{-k*g}}{\sum_{i=1}^N e^{-k*g_i}}$$

where  $g_i$  is the gap for the  $i$ th organism in the population. Thus, changing the selection parameter  $k$ , as in the  $k_+$  and  $k_-$  conditions, changes the scale of the fitness values. Their behavior over time is more important than the scale, but in order to not skew the visualization, the control condition is left off of the fitness plots.

## 4.1. Results

---

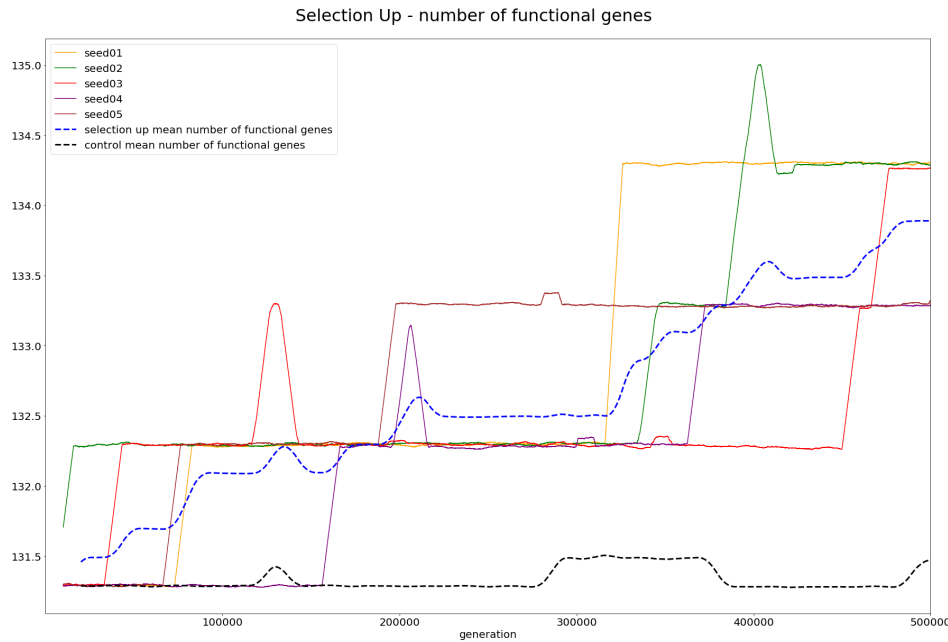


Figure 4.18:  $k_+$  population mean number of functional genes, generations 1-500,000, all seeds.

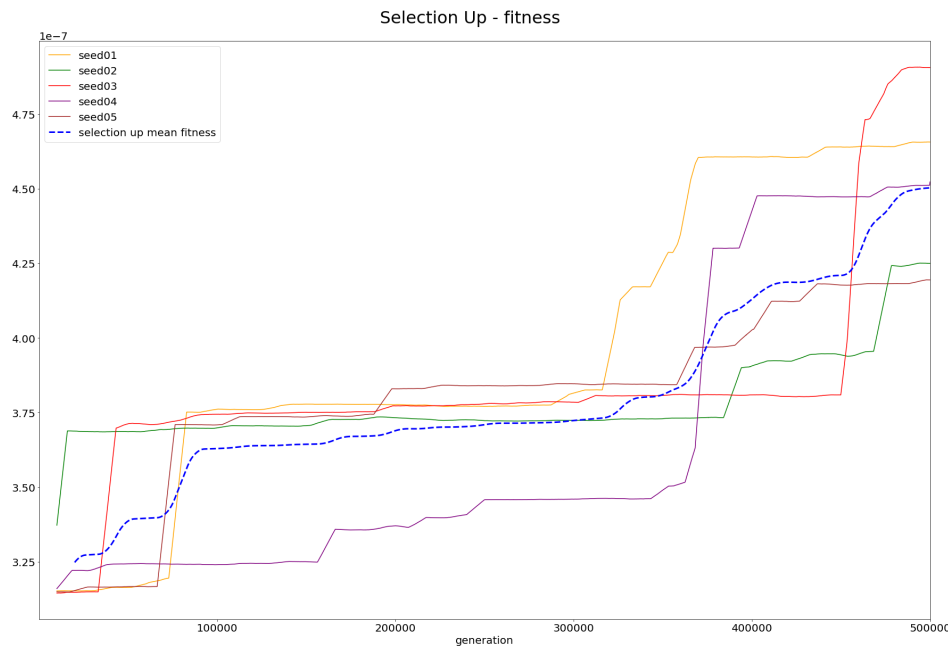


Figure 4.19:  $k_+$  population mean fitness, generations 1-500,000, all seeds.

## 4.1. Results

---

Lastly, Figure 4.20 shows that some of the increased genome size is due to addition of non-coding bases, too.

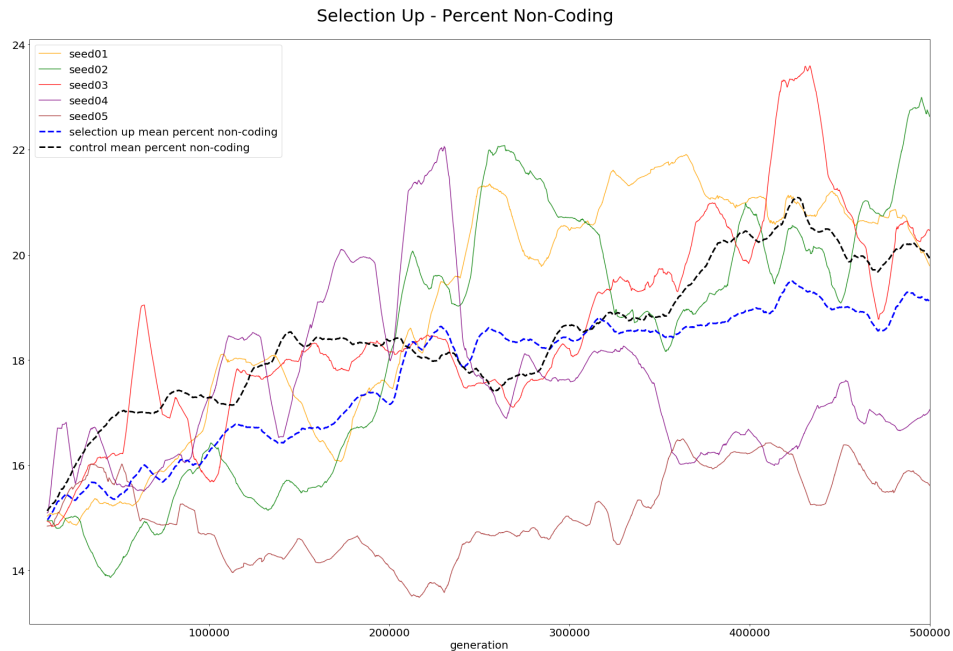


Figure 4.20:  $k_+$  population mean percent non-coding, generations 1-500,000, all seeds.

### 4.1.5 Selection Down

Figure 4.21 shows the genome size results for the  $k_-$  condition.

## 4.1. Results

---

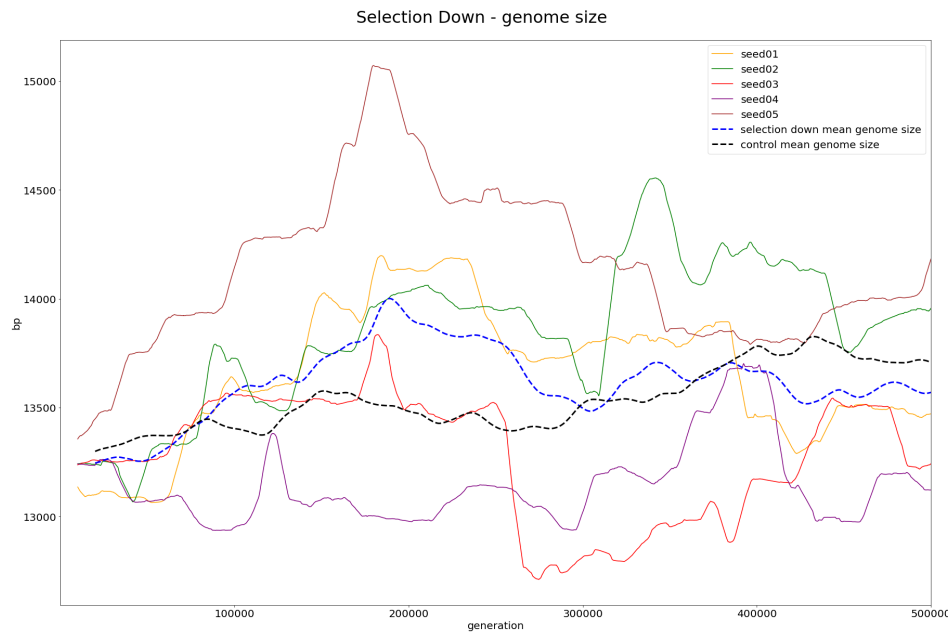


Figure 4.21:  $k_-$  population mean genome size, generations 1-500,000.

The slight increase in genome size is probably best explained by the gaining of some non-coding bases, as shown in Figure 4.22, as the decreased selection caused an overall loss in the number of functional genes for most seeds for most of the generations (see Figure 4.23).

## 4.1. Results

---

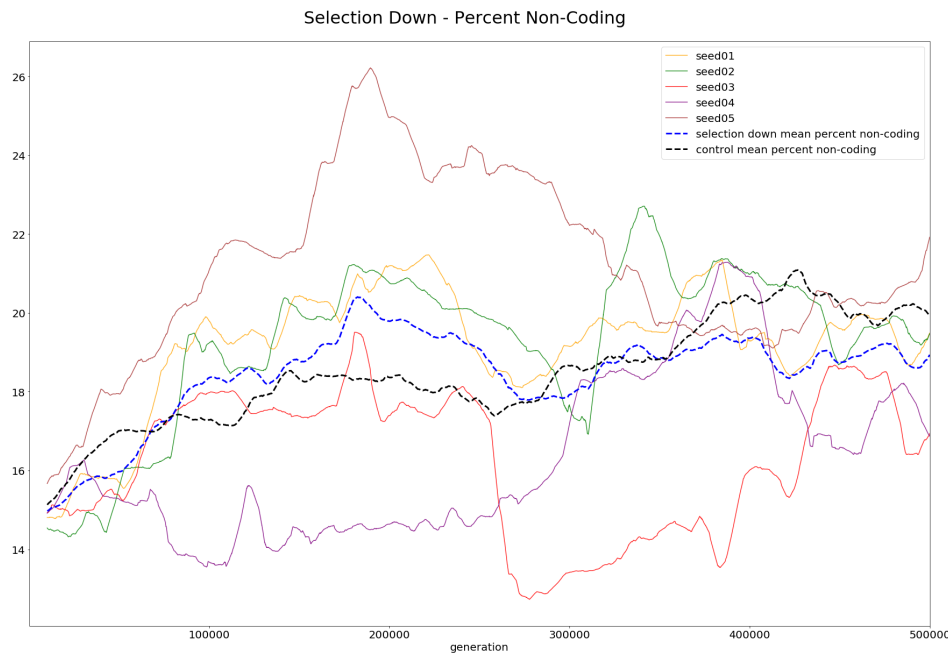


Figure 4.22:  $k_-$  percent non-coding, generations 1-500,000, all seeds.

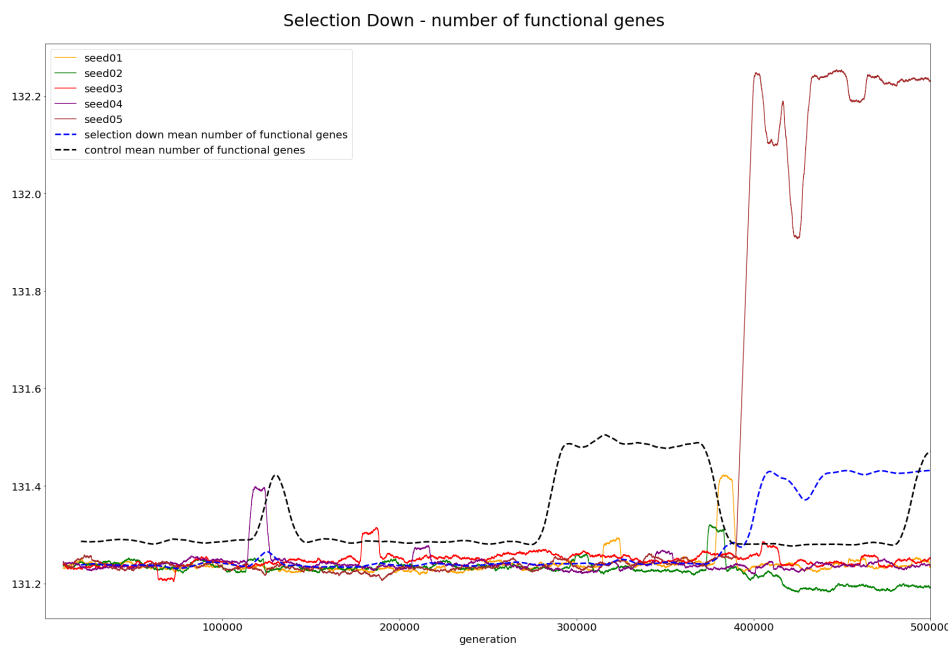


Figure 4.23:  $k_-$  mean population number of functional genes, generations 1-500,000, all seeds.

#### 4.1.6 Population Up

Figure 4.24 shows the mean population genome size for the  $N_+$  condition, and it is clearly the condition which experienced the largest amount of reductive evolution over the course of the 500,000 generations.

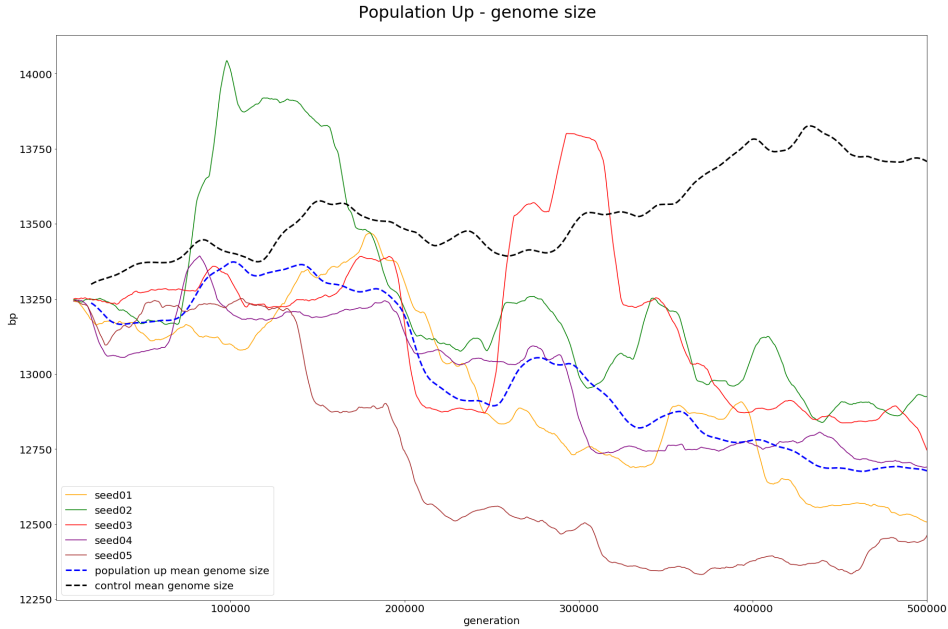


Figure 4.24:  $N_+$  genome size, generations 1-500,000.

Confirming the work of Batut et al. [2], the increased  $N_e$  allowed the efficacy of selection to increase, removing deleterious mutations from the genome, removing non-coding DNA (Figure 4.25).

## 4.1. Results

---

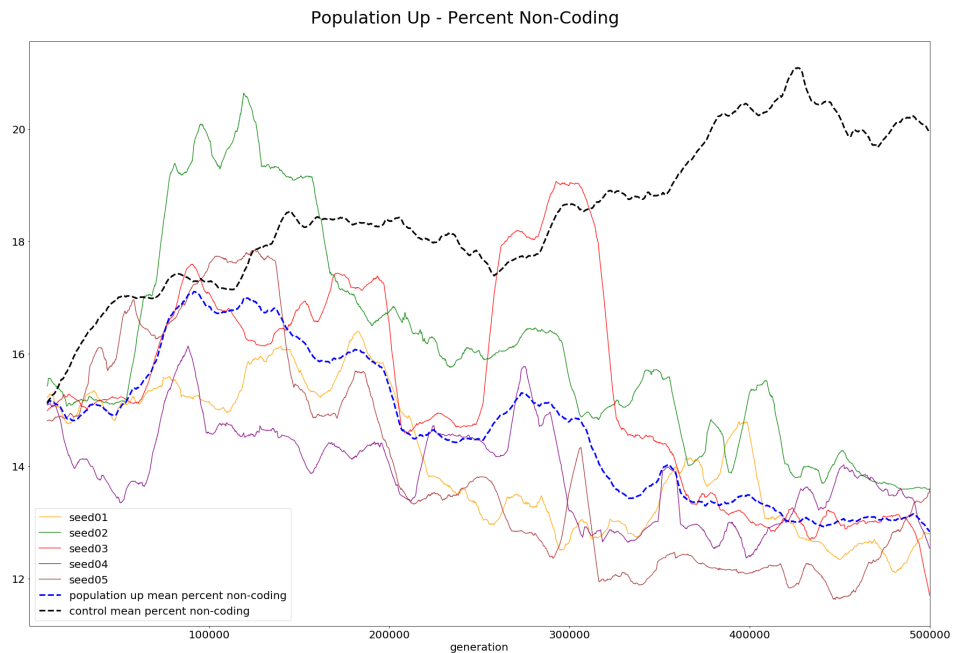


Figure 4.25:  $N_+$  population mean percent non-coding, generations 1-500,000, all seeds.

#### 4.1.7 Population Down

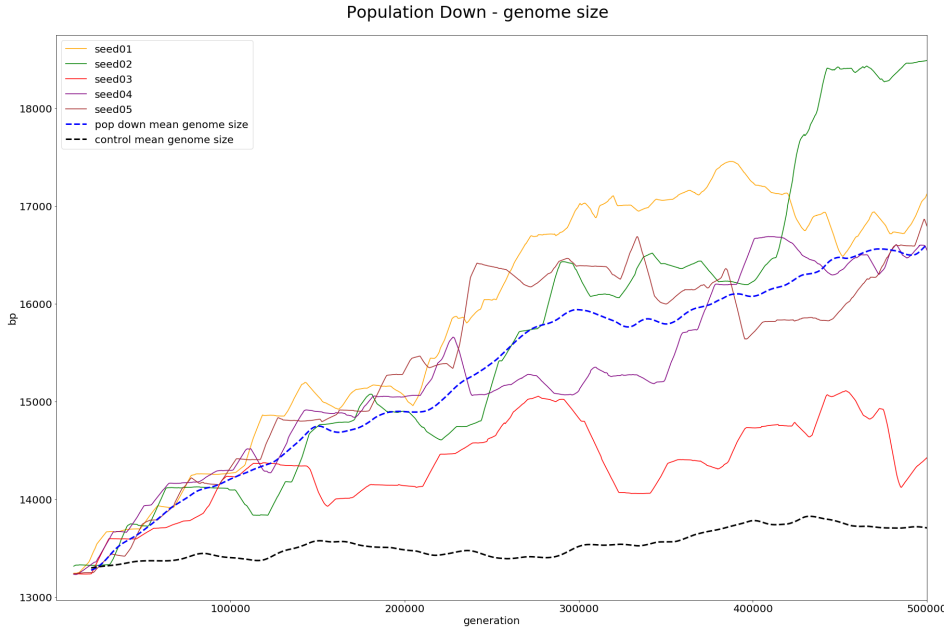


Figure 4.26:  $N_-$  genome size, generations 1-500,000.

The  $N_-$  condition ending up with a genome over 20% larger than the control condition perfectly illustrates the effects of genetic drift described by Batut et al. with regard to small effective population sizes ( $N_e$ ) [2]. The efficacy of selection to remove deleterious mutations and accumulations of non-coding bases is predicted to go down in populations with a smaller effective population size, causing rapid expansion of the genome size. This appears to be exactly what happened here, as Figure 4.27 shows the amount of non-coding bases greatly expanding, reaching 17.7% over the control condition.

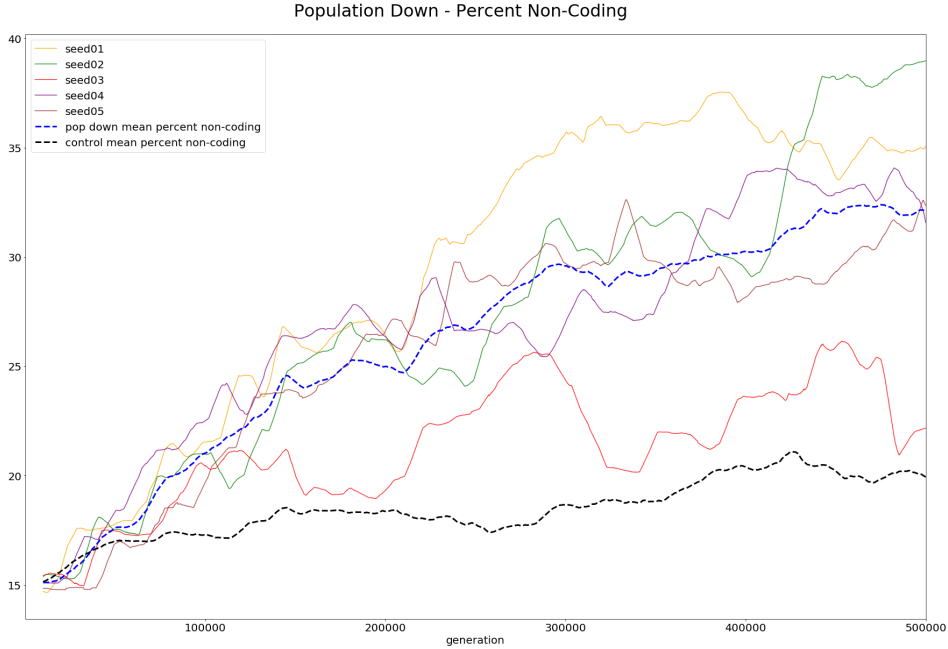


Figure 4.27:  $N_-$  population mean percent non-coding, generations 1-500,000, all seeds.

#### 4.1.8 Statistics and Combined Conditions

In this section, statistics are given for the above conditions and the results are combined into single tables and graphs for ease of comparison. As above, the result are, unless specified otherwise, the mean across all seeds for all 500,000 generations.

#### Genome Size

Figure 4.28 presents the main findings regarding genome size for all conditions. In the figure, the blue line shows the control condition and the other colors show the changed conditions:  $\mu_+/\mu_-$  (mutation up/down),  $k_+/k_-$  (selection up/down), and  $N_+/N_-$  (population up/down). As can be seen from the figure, the expectations from Section 3.4 did not always hold up, as several conditions actually *increased* over their original size.

## 4.1. Results

---

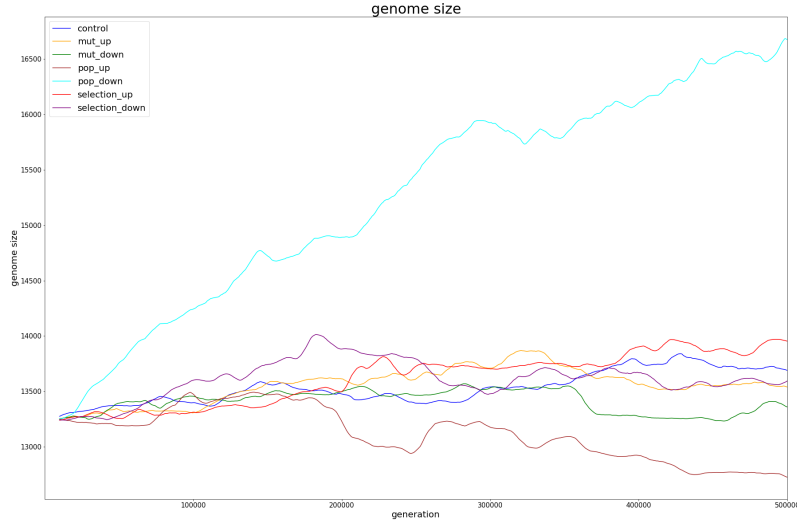


Figure 4.28: Average genome size across the population, in number of bases, of all conditions. Average taken across all five seeds for each condition.

In fact, the  $N_-$  condition had a runaway increase in the number of bases, reaching over 16,500 bases at one time, a 25% increase over the original wild type's roughly 13,200 bp. Even after 500,000 generations, it seems that the upper size limit may still not have been reached. The statistical results are given below in Tables 4.3 and 4.2, which show the mean and standard deviation for all seeds across all 500,000 generations.

Genome Size - 500k Gen. Mean & Std. Dev. (in bp)			
	mean	standard deviation	mean's % change from control
control	13537.031513	144.351	—
$\mu_+$	13558.374160	155.077847	0.157661
$\mu_-$	13410.743690	101.376104	-0.932906
$k_+$	13621.901104	229.635708	0.626944
$k_-$	13614.663599	172.675042	0.573479
$N_+$	13119.243838	230.240517	-3.086258
$N_-$	15275.149392	950.266243	12.839727

Table 4.2: Average genome size across all 500,000 generations, with standard deviation for all seeds and all conditions.

Genome Size - Rank Sum & P-Values		
	rank sum U	p-value
$\mu_+$	110508011469.50	0.00000000
$\mu_-$	71008638349.50	0.00000000
$k_+$	100151680984.50	0.00000000
$k_-$	88533681875.00	0.00000000
$N_+$	21845365773.50	0.00000000
$N_-$	16477791900.50	0.00000000

Table 4.3: Genome size rank sum statistics.

Of the remaining conditions, all but the  $k_+$  condition (which had an increase of 11% over the control condition) ended up with fewer base pairs than the control condition, though all increased slightly over their starting point. Also noteworthy is that the mutation down condition appears to have had a steady increase in the number of base pairs until a maximum of just over 14,000 around generation 350,000 before having a fairly sharp decline back to nearly the original size.

Examining the percent changed from the control condition shown in Figure 4.29 it can be seen that at points, the  $\mu_-$  condition was nearly 5% smaller than the control condition.

## 4.1. Results

---

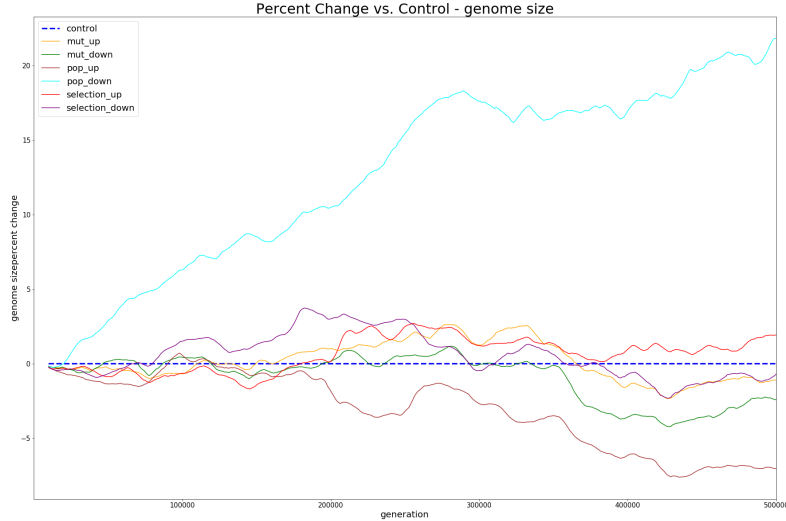


Figure 4.29: Genome size's percent change from the control condition.

Lastly, a zoomed-in look at just the last 50,000 generations is provided in Figure 4.30, allowing a clearer distinction between the control and other conditions. The respective statistics are given in Table 4.4. In the figure, the horizontal dashed black line gives the control condition's genome size at generation 0, the blue dashed line gives the mean genome size across all control seeds, and the colored dashed lines in each figure give the mean of the seeds for that condition.

## 4.1. Results

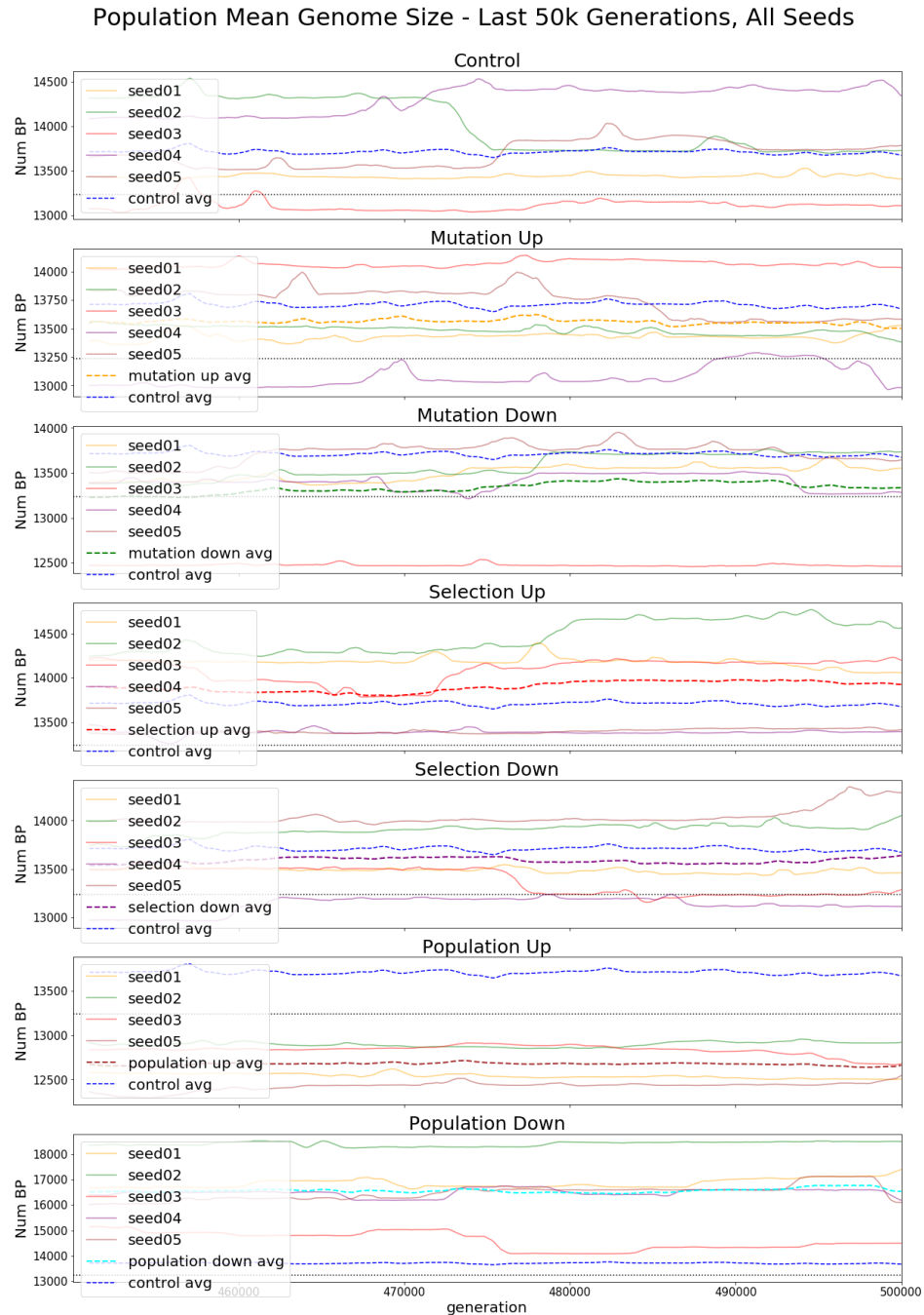


Figure 4.30: Genome Size - Last 50k Generations, all seeds, all conditions. All seeds are shown (colored, solid lines) as well as the mean across all seeds for each condition (colored, dashed lines) are given. The black dashed line is the genome size at generation 0 in the control condition.

<b>Genome Size - Last 50k Gen. Mean &amp; Std. Dev.</b>			
	<b>Mean</b>	<b>Std. Dev</b>	<b>% change from control</b>
control	13710.785821	23.9975	—
$\mu_+$	13560.671469	21.360848	-1.094863
$\mu_-$	13332.739494	61.121661	-2.757291
$k_+$	13901.869266	57.819805	1.393672
$k_-$	13587.959325	27.504289	-0.895838
$N_+$	12680.917724	12.583662	-7.511372
$N_-$	16562.744322	80.705805	20.800839

Table 4.4: This table shows the mean, standard deviation, and percent change from the control condition for the population for just the last 50k generations.

### Metabolic Error and Fitness

Figure 4.31 shows three categories of information for each condition: 1) the mean population fitness for each seed (in various colors), 2) the mean fitness across all seeds for that condition (dashed line, black), and 3) the control condition (dashed line, blue) for each condition.

## 4.1. Results

---

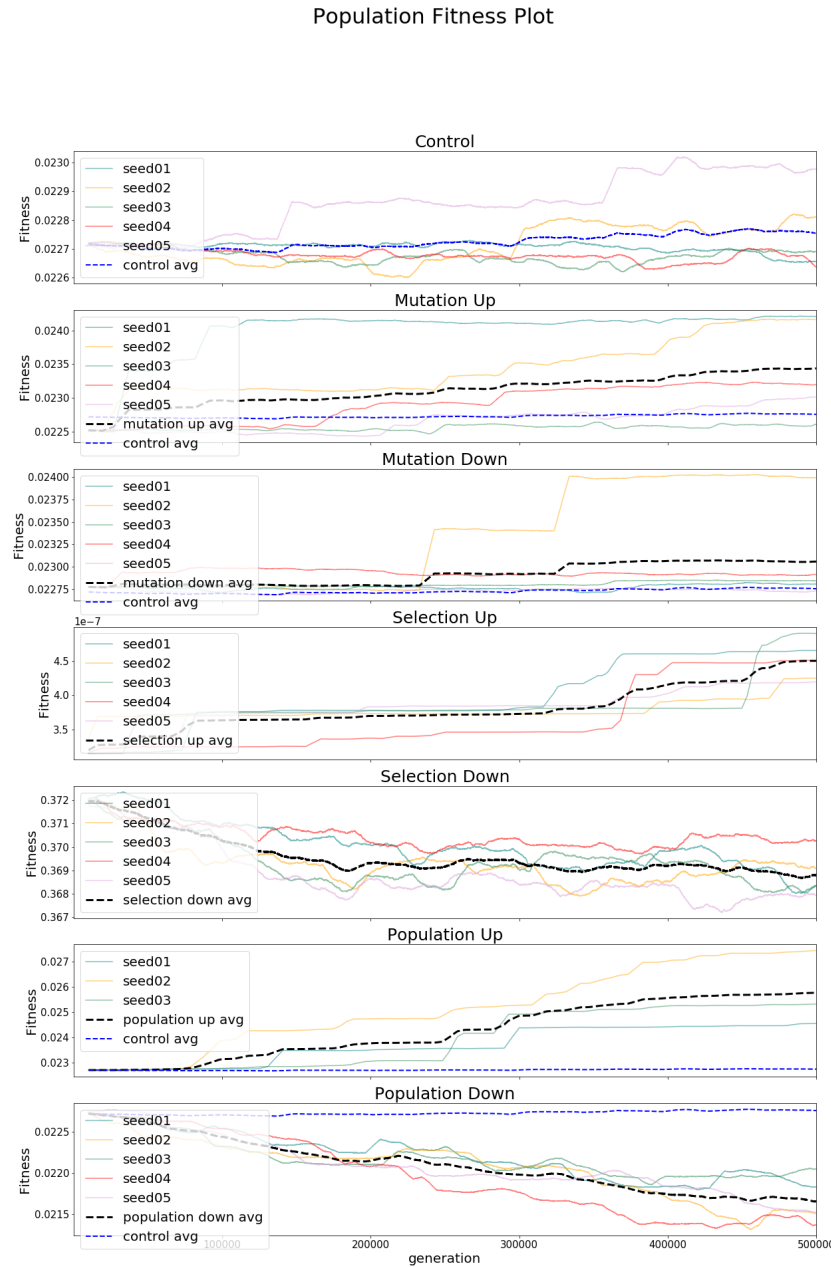


Figure 4.31: Mean population fitness for each condition. All seeds are shown; the average for that condition is shown in black and the control condition is blue.

## 4.1. Results

---

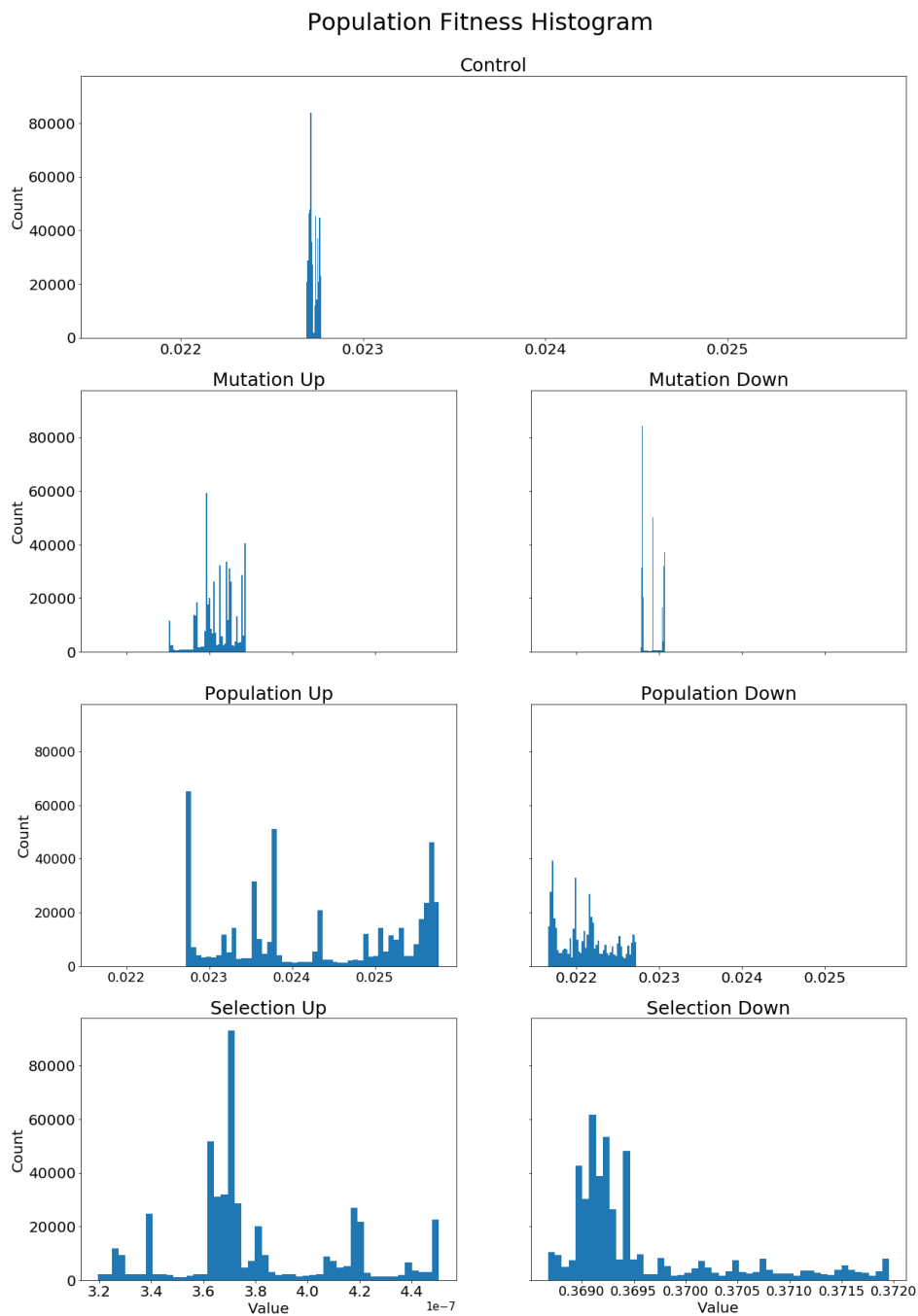


Figure 4.32: Histogram of population fitness at generation 500,000 for all conditions. Note that the x-axes for both the  $k_+$  and  $k_-$  conditions are on a different scale relative to the other conditions and each other.

## 4.1. Results

---

Figure 4.32 shows a histogram of the population mean fitness values for all conditions over the 500k generations. This figure is included to show the relative "stability" of a condition, i.e. to show how many times the fitness changed throughout the simulations. For example, although the  $\mu_-$  condition ended the simulations in the most similar position to the control condition regarding fitness (just 0.8% away), the more even distribution of the value counts for the control condition given in Figure 4.32 makes it clear that the control condition experienced more fluctuations in value throughout the simulation. By contrast, the  $\mu_-$  condition, as expected, tended to hover at certain locations in between rarer mutation events. This directly correlates to evolvability (see Section 4.1.10).

Figure 4.33 shows the mean metabolic error across all seeds for the whole population over time with respect to each condition.

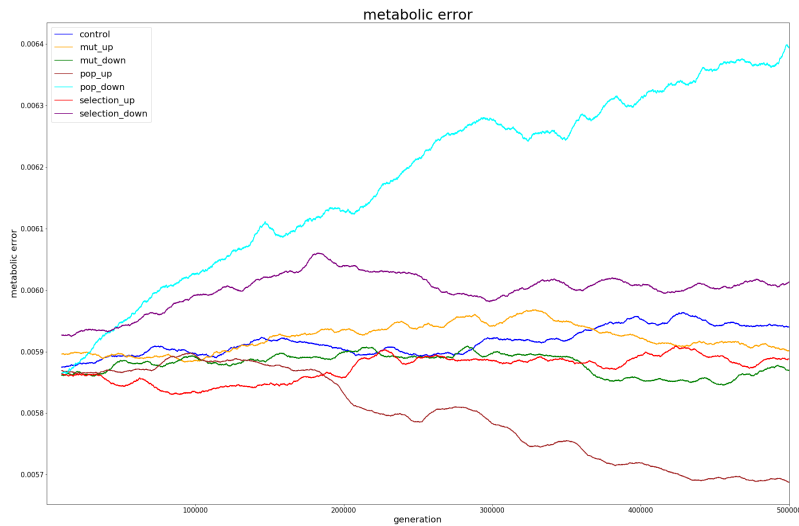


Figure 4.33: Plot of the population mean metabolic error over time for all conditions, average of all seeds

Table 4.5 below gives the mean fitness scores for the population and the differing conditions.

Fitness			
	mean	standard deviation	mean's % change from control
control	2.272542e-02	2.34433e-05	—
$\mu_+$	2.310701e-02	2.191826e-04	1.679131
$\mu_-$	2.290879e-02	1.180940e-04	0.806895
$k_+$	3.803823e-07	3.130504e-08	-99.998326
$k_-$	3.695935e-01	8.101732e-04	1526.344327
$N_+$	2.378802e-02	7.072942e-04	4.675849
$N_-$	2.209722e-02	3.104264e-04	-2.764272

Table 4.5: Population mean fitness, standard deviations, and percent change from the control condition across all seeds.

#### 4.1.9 Genome Structure

In this section, the effects of the differing conditions on the structure of the genome as measured by the criteria in Tables 3.3 and 3.4 is examined.

**Non-coding DNA** One important factor in genome structure is the amount of non-coding DNA, i.e. the number of bases which are part of a genome but which do not encode protein sequences. Aevol gives the number of bases which are not in any coding sequence, as well as the total genome size, so one may easily calculate this percentage. The results from the experiments for all conditions are shown in Figure 4.34. Recalling genome size in Figure 4.28, it seems that as the genome size of the population down condition rapidly expanded, most of those expansions were non-coding.

## 4.1. Results

---

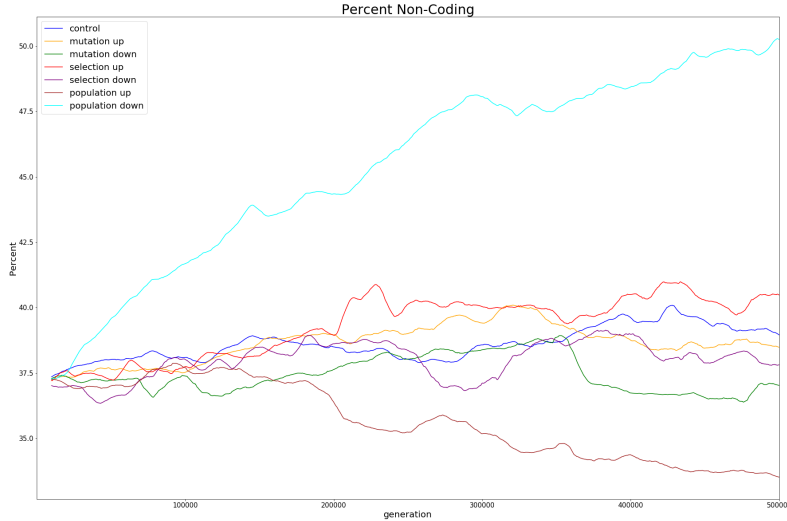


Figure 4.34: Plot of the average (across all seeds) number of non-coding bases for the whole population over time for all conditions.

By comparison, despite the  $k_+$  condition's rapid decline in fitness, it did not acquire more than 1% non-coding DNA.

The average percentages of non-coding DNA are given in Table 4.6 below.

%				Non-coding DNA
	mean	standard deviation	mean's % change from control	
control	38.622711	0.601258	—	
$\mu_+$	38.661764	0.707173	0.101114	
$\mu_-$	37.446414	0.694349	-3.045608	
$k_+$	39.329164	1.138623	1.829114	
$k_-$	38.004029	0.704953	-1.601860	
$N_+$	35.881134	1.519580	-7.098353	
$N_-$	45.462209	3.545778	17.708489	

Table 4.6: Mean and standard deviation of non-coding percentages of DNA across all seeds.

**Number of Functional Genes** Recall from Section 3.2 that a “functional gene” is a gene which produces a gene product. Specifically in Aevol, this means the production of a triangle of mean  $m$ , height  $h$ , and half-width  $w$ . Figure 4.35 below illustrates the mean number of functional genes across the population for each condition.

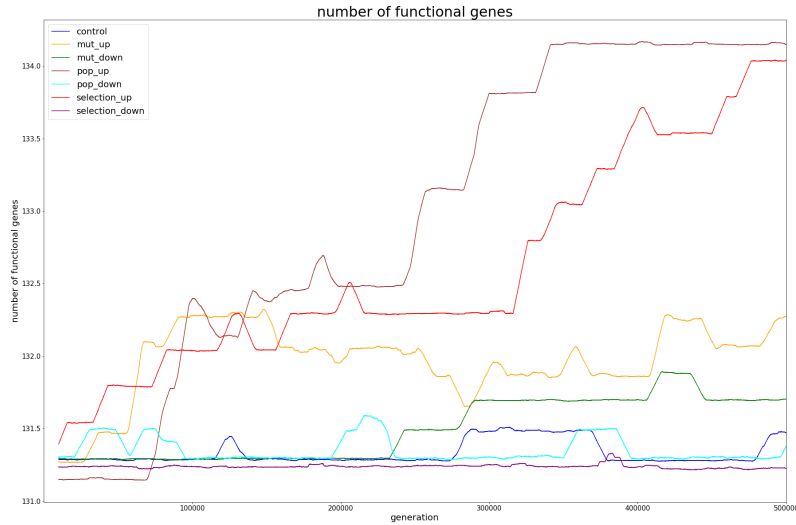


Figure 4.35: Plot showing the mean number of functional genes for the population, averaged across all seeds for each condition.

As seen in Figure 4.35, the  $k_+$  condition showed the greatest increase in the number of functional genes in the whole population, reaching a maximum increase of about 2.2% (131 to 134). This is in agreement with the predictions (from Table 3.5) and the findings of Knibbe et al. [18]. Whereas most of the other curves are fairly flat, the mutation up condition fluctuates relatively rapidly, owing to the quick increase and decrease in the number of base pairs.

The mean and standard deviation of the number of functional genes for the population for each condition is given in Table 4.7 below.

## 4.1. Results

---

### Mean Number of Functional Genes

	mean	standard deviation	% change from control
control	131.332898	0.0815085	—
$\mu_+$	131.974778	0.252463	0.488742
$\mu_-$	131.500541	0.207570	0.127647
$k_+$	132.606568	0.719530	0.969803
$k_-$	131.238909	0.013974	-0.071565
$N_+$	132.378671	0.683269	0.796276
$N_-$	131.350519	0.083280	0.013417

Table 4.7: The mean and standard deviation for the number of functional genes of the population, averaged across all seeds and for all conditions.

**Number of Non-Functional Genes** The average number of non-functional genes across all seeds for each condition is illustrated in Figure 4.36 below, and Table 4.8 provides the mean and standard deviation for all seeds and all conditions.

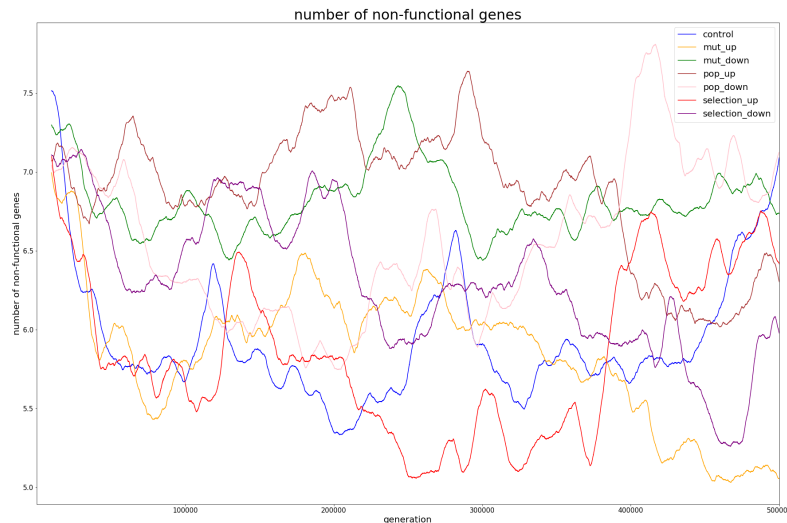


Figure 4.36: The mean number of non-functional genes across all seeds for each condition.

**Mean Num. Non-Functional Genes (Pseudogenes)**  
**Mean & Std. Dev.**

	<b>mean</b>	<b>standard deviation</b>	<b>% change from control</b>
control	5.927067	0.38579	—
$\mu_+$	5.856449	0.428473	-1.191458
$\mu_-$	6.821348	0.221591	15.088075
$k_+$	5.844289	0.506922	-1.396610
$k_-$	6.297804	0.454152	6.254978
$N_+$	6.313992	0.329913	6.528093
$N_-$	6.555471	0.483631	10.602267

Table 4.8: Population mean and standard deviation for the number of non-functional genes, mean of all seeds, all conditions.

**Average Size of Functional Genes** Figure 4.37 shows the average number of base pairs for each functional gene for the population, mapped out over the 500,000 generations. The population down condition continues to be the outlier in terms of genome structure, with the average size of the functional genes remaining noticeably lower than for any other condition. It is worth pointing out, however, that the difference between the smallest average and the largest average is only 1 base pair.

## 4.1. Results

---

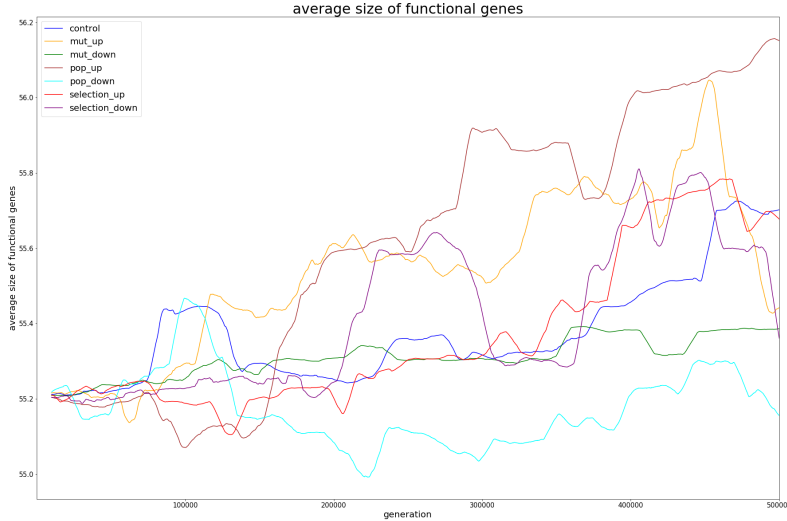


Figure 4.37: Plot showing the average size of functional genes over time for all seeds.

Table 4.9 below summarizes the mean and standard deviation of the average size of functional genes for all conditions, and Table 4.10 gives the p-values for comparing the control condition to every other condition.

### Average size of functional genes

	<b>mean</b>	<b>standard deviation</b>	<b>% change from control</b>
control	55.375430	0.137457	—
$\mu_+$	55.542625	0.207164	0.301929
$\mu_-$	55.309915	0.050594	-0.118309
$k_+$	55.370465	0.202443	-0.008965
$k_-$	55.414465	0.195425	0.070492
$N_+$	55.460664	0.225992	0.153921
$N_-$	55.174290	0.098860	-0.363230

Table 4.9: Mean functional gene size and standard deviation, all seeds, all conditions.

**Average size of functional genes - rank sum & p-value**

	rank sum	p-value
control	124950901896.50	0.36686747
$\mu_+$	68252491056.00	0.00000000
$\mu_-$	96067062201.50	0.00000000
$N_+$	102626876736.00	0.00000000
$N_-$	28963878467.00	0.00000000
$k_+$	103481641646.00	0.00000000
$k_-$	124890321462.00	0.22366471

Table 4.10: Average size of functional genes - rank sum and p-value for all conditions and all seeds.

Since the  $k_-$  condition's p-value was  $\geq 0.05$ , it must be concluded that these results are not significant.

#### 4.1.10 Evolvability

In Figure 4.38 below, the results of the experiments on evolvability for the best individual's (at generation 500,000) lineage are shown.

## 4.1. Results

---

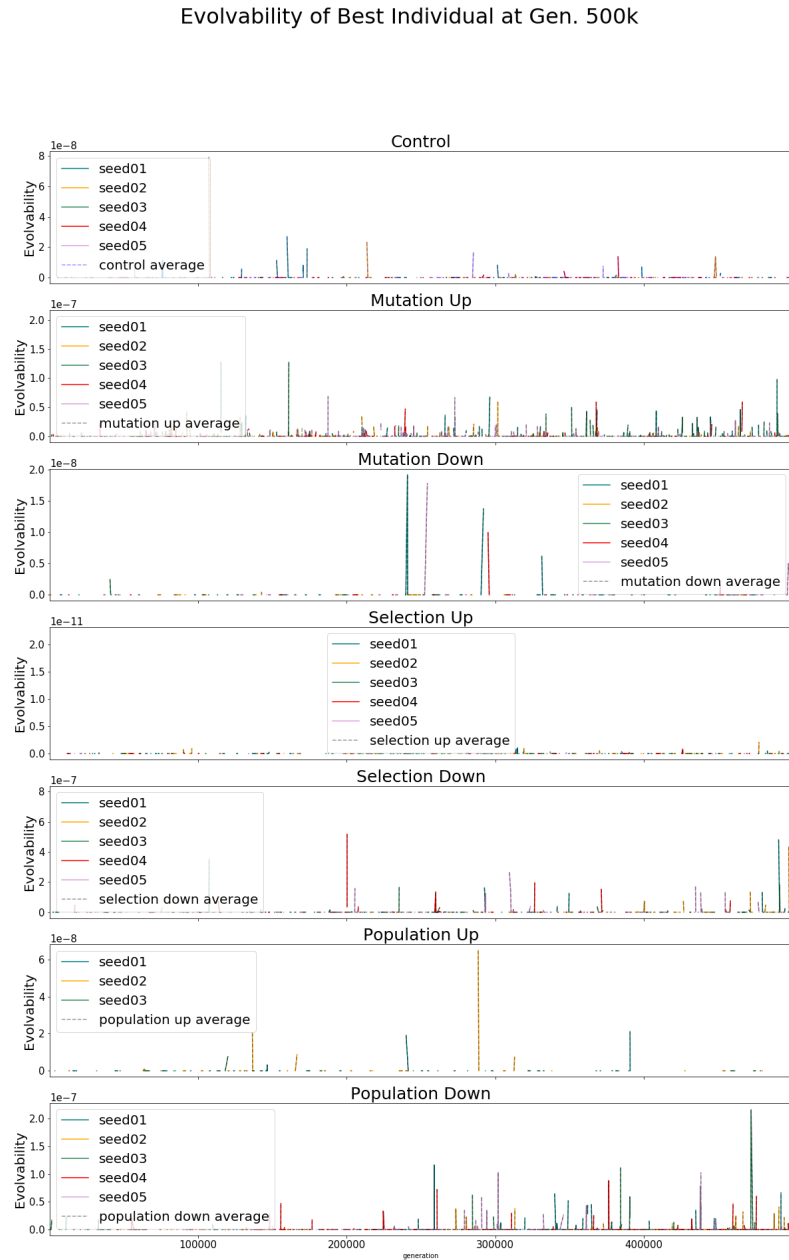


Figure 4.38: A plot showing the evolvability of all seeds and all conditions. Larger numbers are more evolvable (mind the scale for each condition, upper left).

The evolvability rank sum and p-value information is given in Table 4.11.

### Evolvability rank sum and p-value

	rank sum	p-value
$\mu_+$	37476904.00	0.11538726
$\mu_-$	4084573.50	0.00000000
$N_+$	101772759.00	0.00000000
$N_-$	15367560.00	0.00000000
$k_+$	6997351.00	0.00000000
$k_-$	8535654.00	0.00000000

Table 4.11: Rank sum and p-values for evolvability, all seeds, all conditions.

### Evolvability - Mean & Std. Dev.

	mean	standard deviation	% change from control
control	4.133535e-10	3.28521e-09	—
$\mu_+$	1.789394e-09	7.828305e-09	332.8969
$\mu_-$	1.369594e-10	1.320591e-09	-66.86627
$k_+$	4.152320e-14	6.590472e-13	-99.98995
$k_-$	8.394271e-09	5.085889e-08	1930.773
$N_+$	8.149206e-10	4.345602e-09	97.14859
$N_-$	1.015906e-09	8.152163e-09	145.7718

Table 4.12: Table illustrating the mean and standard deviation of the evolvability for each condition.  $\mu$  is the mutation rate,  $k$  is the selection rate, and  $N$  is the population size.

#### 4.1.11 Robustness

Recall from Section 2.1.2 that robustness is measured by the fraction of neutral offspring of an individual. In the following figure, a bar plot showing the spread of neutral offspring for the best individual is seen for the control condition as well as the six variations.

### Robustness - Rank Sum & p-values

	rank sum	p-value
$\mu_+$	6888635.50	0.00000000
$\mu_-$	3858925.50	0.00000000
$k_+$	13792971.00	0.04364015
$k_-$	14320878.00	0.28251799
$N_+$	9467109.50	0.00000000
$N_-$	15908963.00	0.00000000

Table 4.13: Mean robustness rank sum and p-values for all conditions and all seeds.

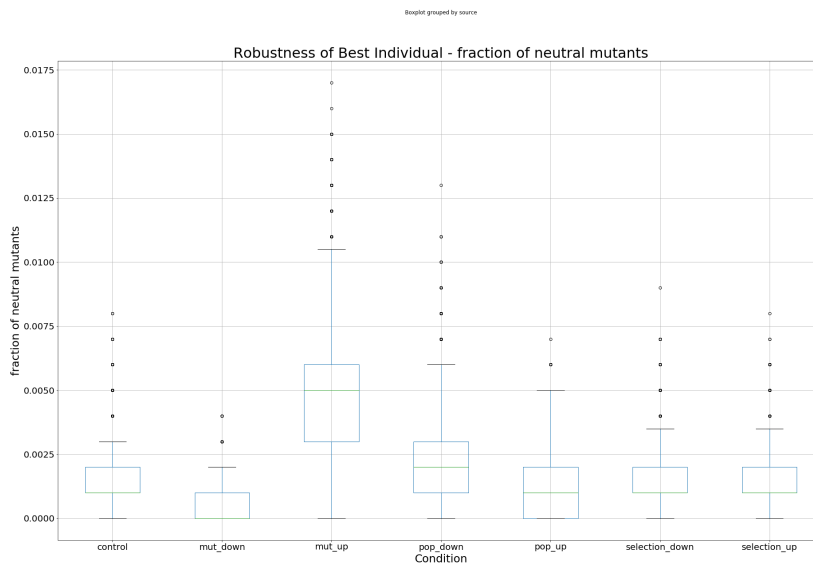


Figure 4.39: A box and whisker plot showing the spread of neutral offspring for the best individual at generation 500,000, all conditions. Higher numbers are more robust.

The mutation up condition clearly had the largest mean percentage of neutral mutants, at 0.5%. The full statistics are given in the tables below. Since the  $k_-$  condition's p-value was  $\geq 0.5$ , it must be rejected.

### Robustness - means & standard deviations

	mean	std. dev.	mean's % change from control
control	0.001470	0.00121821	—
$\mu_+$	0.004852	0.002302	230.026777
$\mu_-$	0.000545	0.000753	-62.935291
$k_+$	0.001427	0.001196	-2.906602
$k_-$	0.001481	0.001215	0.725871
$N_+$	0.001181	0.001106	-19.645748
$N_-$	0.002449	0.001702	66.563607

Table 4.14: Robustness means and standard deviations for all conditions and all seeds.

## 4.2 Discussion

Analogously to Table 3.5, the results of the experiments in Table 4.15 are summarized below. For each cell, green indicates that the prediction was confirmed in these experiments and red indicates that the prediction must be rejected. The predictions for each condition are duplicated here for convenience, with a + indicating a predicted increase and – indicating a predicted decrease over the control condition.

Experiment Results Summary						
Effect On:	Condition					
	$\mu_+$	$\mu_-$	$k_+$	$k_-$	$N_+$	$N_-$
Genome Size	-	+	+	-	-	+
Fitness	+	-	+	-	+	-
Amount of non-coding DNA	-	+	+	-	-	+
Number of genes	-	+	+	-	-	+
Average size of genes	-	+	-	+	-	+
Robustness	-	+	-	+	-	+
Evolvability	+	-	+	-	-	+

Table 4.15: A summary of whether the experiment results confirmed or denied the hypotheses of Table 3.5. were confirmed (green) or rejected (red), along with the predicted results of whether the given result would increase (+) or decrease (-) over the control condition.

According to the predictions based on a survey of the literature (as summarized in Table 3.5), only the  $\mu_+$ ,  $k_-$ , and  $N_+$  conditions were predicted to lead to a reduced genome. As shown in Figure 4.28, however, although the  $\mu_+$  and  $k_-$  conditions did end up with a genome size which was noticeably smaller than the control condition, surprisingly  $\mu_-$  also experienced a reduction in genome size.

The largest driver of reductive evolution in these experiments, as summarized by Table 4.2, was clearly increasing the population size. The efficacy of selection to overcome genetic drift was greatly increased by the availability of greater genetic variance in the larger population. This largely confirms the work of Batut et al. [2].

At first glance, the increase in genome size in the  $\mu_+$  condition seems to counter the prediction based on Liard et al. [21] as discussed in Section 2.6.1. Based on their research, in the  $\mu_+$  condition, an increased mutation rate is expected to boost mutational robustness by disrupting existing genes and introducing many non-coding bases, which in turn allows purifying selection to overcome the proposed complexity ratchet, finally reducing the genome. If one examines the general trends rather than just the final result, it becomes clear that this does seem to be what happened in these experiments, as well,

as the final genome size was below the control condition and seemingly still on its way down. Figure 4.9 confirms that, as time went on, the robustness greatly increased over the control condition (blue dashed line vs. black dashed line) and Figure 4.10 indicates that purifying selection was at work, increasing the gene density. Similarly, Figure 4.11 shows the initial increase in the number of non-coding bases as genes were disrupted.

Given the increase in fitness and gene density in the  $\mu_-$  condition, and the fact that the number of functional genes increased (see Figure 4.14 above), it seems clear that, unlike in real populations where the rate of selection may vary dynamically according to several factors [22], the artificially-steady selection rate of these experiments overcame the natural accumulation of deleterious mutations in favor of a denser genome. The loss of non-coding bases shown in Figure 4.16 confirm this.

Examining Figure 4.31, it quickly becomes apparent that, in the static environment in which the wild type evolved, adding another 500,000 generations on top of the previous 10 million does not much affect the average fitness of the control condition. Small fluctuations occurred due to mutations, insertions, etc. but overall the genotype was quite steady. However, for the  $\mu_+$ ,  $\mu_-$ ,  $k_+$ , and  $N_+$  conditions, a clear trend towards improved fitness may be observed.

More interesting are the  $N_-$  and  $k_+$  conditions, where by generation 500,000 the average fitness in the whole population declined to 2.76% and 99.99% below the control condition respectively (see Table 4.5). It seems that with the smaller population size, genetic drift may be more strongly at work in continually increasing the gap between the phenotype and environmental function, as the lack of variety inherent in a smaller population causes a cascade of increasingly deleterious consequences.

Regarding the  $N_-$  condition, comparing this with the results of Batut et al. and their work with *Buchnera aphidicola* (see Section 2.6), it may be possible that gene loss is occurring because of the smaller effective population size clicking down Muller's ratchet. This does not seem to be what is happening in these experiments either, however. Though mean fitness of the  $N_-$  condition did greatly decline (see Figure ??), the  $N_-$  condition also saw the largest accumulation of non-coding DNA (see Figure 4.34) and the second-highest level of evolvability (see Table 4.12), which should theoret-

ically have lead to an easier time of overcoming the ratchet. On the other hand, the number of functional genes stayed more or less the same as all of the other conditions, and the accumulated number of non-functional genes (pseudogenes) of the  $N_-$  condition was the largest (see Figure 4.36). These two factors together suggest that there almost certainly was some loss of fitness through pseudogenization; perhaps with more time, the pseudogenes would also have been lost.

Recall the work of Liard et al.[21] as discussed in Section 2.6, in which the proposed “complexity ratchet” was overcome by increasing the mutation rate. Their work was quite successful in overcoming this ratchet, but in the experiments of this thesis, both the number of genes and the average size of the genes increased. One possible explanation for this is that, in their work, their increased mutation rate  $\mu_+$  was set to  $1e^{-3}$ . By contrast, even the elevated mutation rate used here,  $\mu_+$ , was just  $4e^{-7}$ , which is  $\frac{1}{4} * e^4 \approx 13.65$  times lower than their highest mutation rate. Perhaps an even higher mutation rate would be sufficient to overcome the power of selection and reduce the genome further.

# Chapter 5

## Conclusions and Future Work

In this chapter, the overall conclusions drawn from the work are summarized. Additionally, some limitations of the experiments are discussed, and a few possibilities for further research are highlighted.

### 5.1 Conclusions

There were four conditions in which, at the conclusion of these experiments in *in silico* experimental evolution, the genome size was smaller than the control condition (see Figure 4.28):  $\mu_+$ ,  $k_-$ ,  $N_+$ , and surprisingly  $\mu_-$ .

Overall, direct selection did not seem to have played much of a role in reducing the genome, again in agreement with Batut et al. [2]. The mean population genome size in the  $k_+$  condition ended up being larger than the control condition, likely because of the accumulation of non-coding bases, and for the  $k_-$  condition, the results were found to not be statistically significant.

Changing the mutation rate had a noticeable impact on genome size, however, largely through the introduction of non-coding sequences ( $\mu_+$ ) or through the loss of non-coding bases ( $\mu_-$ ). The large increase in the level of mutational robustness seen in the  $\mu_+$  condition seemed able to overcome the proposed “complexity ratchet” of Liard et al. [21], increasing robustness by 230% (see Table 4.14) while reducing the genome by about 1.1% (see Table 4.3). The steady selection pressure in the  $\mu_-$  condition allowed selection to “keep up” with the random insertions of non-coding bases, eventually

removing them and reducing the overall population mean genome size by 2.76%.

Though it is very unlikely that any single factor can single-handedly lead to reductive genome evolution, based on the results of these experiments, the single largest driver of reductive genome evolution in these scenarios does seem to be effective population size ( $N_e$ ), which was able to reduce the population mean genome size by 7.5% by the last 50,000 generations (see Table 4.3). As discussed by Batut et al. [2], the increased effective population size appears to increase the efficacy of selection to reduce the genome via the removal of non-coding bases and superfluous genes, while at the same time increasing the overall fitness. The average size of coding sequences grew smaller, there were fewer non-coding bases, and the mean number of functional genes increased almost as much as in the  $k_+$  condition, all without the requisite fitness loss. In other words, the genomes become more dense but fitness was not affected, strong characteristics of effective reductive genome evolution.

## 5.2 Relation to Real-World Organisms

This thesis was begun with the goal of examining the factors that may drive reductive evolution, with the overall intention of relating this to real-world examples. The marine cyanobacteria *Prochlorococcus* has large effective population sizes and high adaptability, which has resulted in a large number of ecotypes which exist at differing depths in the oligotrophic oceans. Some possible reasons for this large reduction in genome size for *Prochlorococcus* were examined in Batut et al.[2] and there, the most robust explanation for genomic reduction in *Prochlorococcus* was found to be adaptation to the environment, as the benefit of losing specific cellular machinery for multiple different environments likely outweighed the cost of maintaining them. The experimental results here seem to confirm this hypothesis, as the highly stable environment seems to have allowed the artificial organisms to shed superfluous genes over time, all the while gaining fitness. The larger effective population size of the  $N_+$  condition clearly showed the largest increase in reductive evolution

The fittest organisms overall were those in the  $k_-$  condition. It was

hypothesized in Knibbe et al. [18] and Batut et al. [3] that with decreased selection, the accompanying loss of non-coding bases (and thus a reduction in the genome size) might also cause an increase in fitness, and this was borne out by these experiments. Not only was the  $k_-$  condition the condition with the best fitness, but it also saw the second largest decrease in non-coding bases.

### 5.3 Limitations and Future work

A number of limitations are associated with this work and they are briefly presented here.

#### 5.3.1 Experimental Design Limitations

Although it was the main design of these experiments, one limitation to consider is that only one parameter varied per condition. It seems reasonable to assume that under a combination of conditions, reductive evolution more reliably occurs. Since an increased mutation rate, decreased selection pressure, and an increased population size all lead to a reduced genome in the experiments, it may be worth testing whether a combination of the three would lead to an even greater reduction.

In a similar vein, only one value for each changed condition was tested. For example, only a mutation rate of  $\mu = 4e^{-7}$  was tested for the  $\mu_+$  condition. Perhaps an even higher mutation rate might be enough to further reduce the number of genes, as predicted by Knibbe et al. [18] and [21]. Their mutation rates were  $2.1e^{-5}$  and  $1e^{-3}$  respectively, roughly 3.9 and 13.65 times higher than the rate found here. The testing of more extreme values for each parameter may provide a fuller picture of the balance between selection, mutation rates, population sizes, and reductive genome evolution. As further evidence of the potentially limiting rate of mutation used in these experiments, when examining the work of Knibbe et al. regarding “successful” genomes requiring mostly neutral or beneficial offspring (see Section 2.6), the link between a greater increase in the mutation rate (and thus mutational robustness) and genome reduction bears further research.

Another limitation is that the environments did not vary in these experiments. Aevol includes the ability to vary the environment natively, so future

experiments could vary the environment over time to see if doing so would increase or decrease robustness or evolvability, which are strong drivers of reductive evolution [3].

### 5.3.2 Limitations of the Aevol Model

Aevol as a modeling software is limited in that, like all models, it relies on several simplifications. For example, the population sizes tested here, even in the population up condition where  $N = 4096$ , are still much smaller than would be found in real world bacterial populations. It has been estimated that some reduced *Prochlorococcus* populations may have an effective population size of  $N_e \cong 10^9$  [16]. It could be that in order to properly judge the effects of Muller’s ratchet under differing conditions, for example, much larger population sizes are needed. However, the length of time required for running such a simulation in Aevol even on a decent cluster might make this intractable, as quadrupling the population size for the  $N_+$  condition also greatly increased the run-time of these experiments. Currently, running the simulation with even 4096 organisms for 500,000 generations required over five days of computation time on a 96-core cluster. Future versions of Aevol may see more optimization, but simulating population sizes on the order of magnitude of *Prochlorococcus*’ estimated effective population size currently remains a daunting task.

Another limitation of the Aevol model is that, as mentioned in Section 4.1.8, non-coding DNA has no associated fitness costs in Aevol. In real-world bacteria, replicating non-coding DNA has a certain cost, as the resources required for these bases must still be procured and a certain amount of energy expended for the replication. Nevertheless, there is indirect selection pressure associated with non-coding DNA, as Knibbe et al. showed, because “varying the amount of nonfunctional DNA would not change the immediate fitness of the organism but would rather modify the chance that its offspring retain it” [18].

Lastly, Aevol also relies on the simplification that its space of “biological functions” are a one-dimensional function, when the real-world space is obviously much more complicated. Mapping real-world biological functions to a one-dimensional space is difficult enough in and of itself, but this simplification also effectively disallows the use of gene networks, which may be

### 5.3. Limitations and Future work

an important factor in determining which genes are lost in reductive evolution [40]. Similarly, Aevol is also limited in its representation of pleiotropy (a single gene influencing two or more phenotypic traits). In Aevol, a protein can perform several functions but these functions must necessarily be functionally close together, as their requisite bases are close on the possibility axis. In real organisms, however, a single protein can perform very different functions; this may influence gene loss events as well, given the typically dense nature of bacterial genomes, *Prochlorococcus* being no exception.





# Bibliography

- [1] Thomas Bataillon. Estimation of spontaneous genome-wide mutation rate parameters: whither beneficial mutations? *Heredity*, 84(5):497–501, 2000.
- [2] Bérénice Batut, Carole Knibbe, Gabriel Marais, and Vincent Daubin. Reductive genome evolution at both ends of the bacterial population size spectrum. *Nature reviews. Microbiology*, 12(12):841–850, 2014.
- [3] Bérénice Batut, David P. Parsons, Stephan Fischer, Guillaume Beslon, and Carole Knibbe. In silico experimental evolution: a tool to test evolutionary scenarios. *BMC bioinformatics*, 14 Suppl 15:S11, 2013.
- [4] Guillaume Beslon, Vincent F Liard, and Santiago F Elena. Testing evolution predictability using the aevol software. 16th international meeting of the European Society of Evolutionary Biology (ESEB 2017), August 2017. Poster.
- [5] Katie Bradwell, Marine Combe, Pilar Domingo-Calap, and Rafael Sanjuán. Correlation between mutation rate and genome size in ri-boviruses: mutation rate of bacteriophage q $\beta$ . *Genetics*, 195(1):243–251, 2013.
- [6] John FY Brookfield. Evolution and evolvability: celebrating darwin 200. *Biology letters*, 5(1):44–46, 2009.
- [7] Quentin Cardé, Marco Foley, Carole Knibbe, David P Parsons, Jonathan Rouzaud-Cornabas, and Guillaume Beslon. How to reduce

a genome? alife as a tool to teach the scientific method to school pupils. In *The 2018 Conference on Artificial Life: A Hybrid of the European Conference on Artificial Life (ECAL) and the International Conference on the Synthesis and Simulation of Living Systems (ALIFE)*, pages 497–504. MIT Press, 2019.

- [8] Clarence FG Castillo and Maurice HT Ling. Digital organism simulation environment (dose): A library for ecologically-based in silico experimental evolution. *Advances in Computer Science : an International Journal*, 3(1):44–50, 2014.
- [9] A.D. Cutter. *A Primer of Molecular Population Genetics*. Oxford University Press, 2019.
- [10] Carolina Díaz Arenas and Tim F. Cooper. Mechanisms and selection of evolvability: experimental evidence. *FEMS Microbiology Reviews*, 37(4):572–582, 07 2013.
- [11] Robert W Doran. The gray code. *J. UCS*, 13(11):1573–1597, 2007.
- [12] John W Drake. A constant rate of spontaneous mutation in dna-based microbes. *Proceedings of the National Academy of Sciences*, 88(16):7160–7164, 1991.
- [13] Alexis Dufresne, Laurence Garczarek, and Frédéric Partensky. Accelerated evolution associated with genome reduction in a free-living prokaryote. *Genome biology*, 6(2):R14, 2005.
- [14] Santiago F Elena, Claus O Wilke, Charles Ofria, and Richard E Lenski. Effects of population size and mutation rate on the evolution of mutational robustness. *Evolution*, 61(3):666–674, 2007.
- [15] Isabel Gordo and Brian Charlesworth. On the speed of muller’s ratchet. *Genetics*, 156(4):2137–2140, 2000.
- [16] Nadav Kashtan, Sara E Roggensack, Sébastien Rodrigue, Jessie W Thompson, Steven J Biller, Allison Coe, Huiming Ding, Pekka Marttinen, Rex R Malmstrom, Roman Stocker, et al. Single-cell genomics reveals hundreds of coexisting subpopulations in wild prochlorococcus. *Science*, 344(6182):416–420, 2014.

- [17] Carole Knibbe. *Evolution of genome structure by indirect selection of the mutational variability: a computational approach*. Theses, INSA de Lyon, December 2006.
- [18] Carole Knibbe, Antoine Coulon, Olivier Mazet, Jean-Michel Farray, and Guillaume Beslon. A long-term evolutionary pressure on the amount of noncoding dna. *Molecular Biology and Evolution*, 24(10):2344–2353, 08 2007.
- [19] Sanna Koskineni, Song Sun, Otto G Berg, and Dan I Andersson. Selection-driven gene loss in bacteria. *PLoS genetics*, 8(6), 2012.
- [20] Chih-Horng Kuo, Nancy A Moran, and Howard Ochman. The consequences of genetic drift for bacterial genome complexity. *Genome research*, 19(8):1450–1454, 2009.
- [21] Vincent Liard, David Parsons, Jonathan Rouzaud-Cornabas, and Guillaume Beslon. The complexity ratchet: Stronger than selection, weaker than robustness. *Artificial Life Conference Proceedings*, 1(30):250–257, 2018.
- [22] Michael Lynch, Matthew S Ackerman, Jean-Francois Gout, Hongan Long, Way Sung, W Kelley Thomas, and Patricia L Foster. Genetic drift, selection and the evolution of the mutation rate. *Nature Reviews Genetics*, 17(11):704, 2016.
- [23] Michael Lynch and John S. Conery. The origins of genome complexity. *Science*, 302(5649):1401–1404, 2003.
- [24] Gabriel AB Marais, Alexandra Calteau, and Olivier Tenaillon. Mutation rate and genome reduction in endosymbiotic and free-living bacteria. *Genetica*, 134(2):205–210, 2008.
- [25] Octavio Miramontes, Franois Taddei, Ariel B. Lindner, Antoine Frenoy, and Dusan Misevic. Shape matters in cooperation. *Artificial Life Conference Proceedings*, 1(28):340–341, 2016.
- [26] Dusan Misevic, Antoine Frenoy, David P Parsons, and Francois Taddei. Effects of public good properties on the evolution of cooperation. In

*Artificial Life Conference Proceedings 12*, pages 218–225. MIT Press, 2012.

- [27] J Jeffrey Morris, Richard E Lenski, and Erik R Zinser. The black queen hypothesis: evolution of dependencies through adaptive gene loss. *MBio*, 3(2):e00036–12, 2012.
- [28] Vadim Mozhayskiy and Ilias Tagkopoulos. Microbial evolution in vivo and in silico: methods and applications. *Integrative Biology*, 5(2):262–277, 10 2012.
- [29] H. J. Muller. Some genetic aspects of sex. *The American Naturalist*, 66(703):118–138, 1932.
- [30] C. Ofria and C. O. Wilke. Avida: A software platform for research in computational evolutionary biology. *Artificial Life*, 10(2):191–229, 2004.
- [31] David Parsons. *S ’e indirect election in é Darwinian evolution: m ’e mechanisms and implications*. PhD thesis, Lyon, INSA, 2011.
- [32] T. S. Ray and J. Hart. Evolution of differentiated multi-threaded digital organisms. In *Proceedings 1999 IEEE/RSJ International Conference on Intelligent Robots and Systems. Human and Environment Friendly Robots with High Intelligence and Emotional Quotients (Cat. No.99CH36289)*, volume 1, pages 1–10 vol.1, 1999.
- [33] Gabrielle Rocap, Frank W Larimer, Jane Lamerdin, Stephanie Malfatti, Patrick Chain, Nathan A Ahlgren, Andrae Arellano, Maureen Coleman, Loren Hauser, Wolfgang R Hess, et al. Genome divergence in two prochlorococcus ecotypes reflects oceanic niche differentiation. *Nature*, 424(6952):1042–1047, 2003.
- [34] Jacob Rutten, Paulien Hogeweg, and Guillaume Beslon. Adapting the engine to the fuel: mutator populations can reduce the mutational load by reorganizing their genome structure. *BMC Evolutionary Biology*, 19, 12 2019.
- [35] Lynn Sagan. On the origin of mitosing cells. *Journal of theoretical biology*, 14(3):225–IN6, 1967.

- [36] Yolanda Sanchez-Dehesa, Loïc Cerf, Jose Maria Pena, Jean-François Boulicaut, and Guillaume Beslon. Artificial Regulatory Networks Evolution. In *Proc 1st Int Workshop on Machine Learning for Systems Biology MLSB 07*, pages 47–52, Evry, France, September 2007.
- [37] Ali R Vahdati, Kathleen Sprouffske, and Andreas Wagner. Effect of population size and mutation rate on the evolution of rna sequences on an adaptive landscape determined by rna folding. *International journal of biological sciences*, 13(9):1138, 2017.
- [38] Andreas Wagner. Robustness and evolvability: a paradox resolved. *Proceedings of the Royal Society B: Biological Sciences*, 275(1630):91–100, 2008.
- [39] Tanita Wein and Tal Dagan. The effect of population bottleneck size and selective regime on genetic diversity and evolvability in bacteria. *Genome biology and evolution*, 11(11):3283–3290, 2019.
- [40] Jennifer L Wilcox, Helen E Dunbar, Russell D Wolfinger, and Nancy A Moran. Consequences of reductive evolution for gene expression in an obligate endosymbiont. *Molecular microbiology*, 48(6):1491–1500, 2003.
- [41] Claus O Wilke, Jia Lan Wang, Charles Ofria, Richard E Lenski, and Christoph Adami. Evolution of digital organisms at high mutation rates leads to survival of the flattest. *Nature*, 412(6844):331–333, 2001.